Universidade de Coimbra

Faculdade de Ciências e Tecnologia

Neural correlates of synthetic face and object processing: EEG/ERP and fMRI studies

Investigação das etapas de processamento visual de faces sintéticas ("Mooney Faces") no cérebro e implicação destas no processamento de faces e objectos.

João Miguel Seabra Castelhano

Mestrado Integrado em Engenharia Biomédica

2008

Universidade de Coimbra

Faculdade de Ciências e Tecnologia

Neural correlates of synthetic face and object processing: EEG/ERP and fMRI studies

Investigação das etapas de processamento visual de faces sintéticas ("Mooney Faces") no cérebro e implicação destas no processamento de faces e objectos.

João Miguel Seabra Castelhano

Mestrado Integrado em Engenharia Biomédica

2008

This thesis is presented to the University of Coimbra with the purpose to conclude the Master degree in Biomedical Engineering. All the work was done in **IBILI** - Institute of Biomedical Research on Light and Image with scientific orientation and supervision of Professor Miguel Castelo Branco and José Rebola.

Acknowledgements

This work would not be the same without the brilliant guidance and coordination of my supervisor Professor Miguel Castelo Branco. I thank not only the time available, but any assistance, commitment and motivation in this and other projects.

I am also fully aware of the importance of the support provided by José Rebola. During this year we worked together and I thank the many hours to solve problems, to prepare experiences, to analyse data, to finally learn together. I acknowledge here that all functional magnetic resonance imaging (fMRI) experiments results presented here are the fruit of his work. I know that he left his experiences with “strangely named novel” objects to devote some of his time to the Mooney faces project.

It is also fair to point out Dr. Alda of the Radiology department of HUC who was always available to help us during our experiments.

Concerning our experiments, I have to thank all those who participated as participants either in fMRI experiments or in Electroencephalography (EEG) recordings, because without them none of this would have been possible.

I have an appreciation to Dr. Eugenio Rodriguez from Catholic University of Chile, who released its toolbox “globales” to our analysis of gamma-band power and phase synchrony in EEG and gave as well very important tips for the success of this work.

I can not forget the good / fun environment created with colleagues from IBILI, particularly between-colleagues - help.

And since five years is already some time, I leave a thank you to all my colleagues but especially the friends that I have made and that were with me throughout these years. To my lunch companions I do not thank but I recall the discussions that helped, no doubt, approaching people and strengthen friendships even further.

I would also like to thank all the other friends and my brother but now it seems imperative to thank those who make this possible - my Parents.

Resumo

Vários tipos de paradigmas têm vindo a ser utilizados para o estudo do reconhecimento humano de faces e objectos. Esta área tem recebido considerável atenção nos últimos anos e os “Mooney stimuli” apresentam-se como de particular interesse para perceber o processo de reconhecimento. Estes estímulos, são estímulos visuais e consistem em imagens discretizadas a dois níveis, preto e branco, de tal forma modificadas que mesmo com a pouca informação disponível ainda se consegue reter a informação suficiente para que possam ser discriminados nelas os objectos que as compõem. De particular interesse são as “Mooney faces” onde, mesmo com estas limitações, é possível discriminar uma cara na imagem.

O estudo da resposta e do processamento cerebral a este tipo de estímulo é, na nossa opinião, um bom método para tentar perceber os mecanismos pelos quais o ser humano faz o reconhecimento de faces e objectos sendo ainda possível identificar as características da imagem que permitem tal reconhecimento. O facto de a mesma imagem poder ser percebida como face num determinado ponto do tempo e não o ser noutro instante, permite assim separar etapas de processamento específicas para caras, de outros mais baixos níveis de processamento que não estão relacionados com caras.

Com os resultados deste estudo pretendemos elucidar a natureza da conectividade funcional, nomeadamente a influência de processos “top-down” entre áreas cerebrais activas no processamento de estímulos visuais, especialmente entre o córtex pré-frontal e áreas temporais relacionadas com o processamento visual de alto nível.

Realizámos estudos de Electroencefalografia (potenciais evocados) e Ressonância Magnética funcional, numa tarefa de detecção/percepção de “Mooney faces”. Ao contrário de estudos anteriores em que se compara faces contra outros estímulos diferentes, aqui conseguimos manipular o tempo de detecção/percepção do estímulo por rotação gradual da “Mooney face” da posição invertida para a posição vertical.

A análise dos potenciais evocados, da “time-frequency”, da sincronização e das regiões de interesse, sobre os dados recolhidos, foi a estratégia adoptada para tentar perceber/discernir as correlações neuronais dos mecanismos de decisão no ser humano.

No que diz respeito ao EEG/ERP aparece uma negatividade que parece traduzir o potencial N170 característico para faces e actividade elevada na banda gama de

frequências (60-70Hz) momentos antes de o participante responder ao perceber a cara. A análise de frequências revela ainda que a actividade cobre todo o escalpe, começando em regiões occipitais (mais posteriores) migrando depois para regiões mais parieto-frontais (anteriores). Aparece ainda actividade elevada na análise da "phase-synchrony" numa banda de frequências mais baixas (30-45Hz) mas também antes da resposta, no entanto, esta actividade difere conforme o conjunto de eléctrodos escolhido para a análise. Nesta análise do sincronismo não observámos assimetrias entre hemisférios mas aparece sincronização inter-hemisférica assim como padrões de sincronização ventral/dorsal relacionados com a percepção.

No que diz respeito aos dados funcionais da ressonância, identificámos uma rede de áreas envolvidas no processo geral de tomada de decisão e também um conjunto de regiões que aparecem mais especificamente relacionadas com a decisão perceptual para "Mooney faces".

Abstract

The recognition of human faces and objects has received considerable attention in recent years. For its study various types of paradigms have been used. “Mooney stimuli” are visual stimuli consisting of images rendered in just two colour levels, black and white, which still retain the sufficient information for the objects attached to them to be perceived.

Of particular interest among this type of visual stimulus are the “Mooney faces”, in which the perceptual image of a face emerges despite the restricted information available.

The study of brain processing and response to such stimuli is, in our opinion, relevant to understand the mechanisms by which humans can recognize faces and objects, being thus possible to identify which components or key features of the image lead to such recognition. In particular, we can use these stimuli to separate low level sensory processing that is not related to face features, from aspects that are specifically related to face processing. This is due to the fact that the same image can at distinct times points be or not perceived as a face.

The findings of this study do hopefully also elucidate the nature of functional connectivity, namely "top-down" influence between brain areas in the processing of visual stimuli, especially between the pre-frontal cortex and the temporal areas related to high level visual processing.

Here we perform Electroencephalography/Event Related Potential measurements (EEG/ERP) and functional Magnetic Resonance Imaging (fMRI) studies in a Mooney face detection task. Previous studies on Mooney stimuli have focused on comparing faces vs. non-faces, using different stimuli [1]. Now we manipulate time to detection of the same stimulus through gradual stimulus rotation from inverted to upright in a face perception task.

Event related potential (ERP), time-frequency and phase synchrony analysis of EEG data and whole-brain region of interest (ROI) analysis of neuroimaging data were carried out. This strategy was tuned to help dissect the neural correlates of perceptual decision making.

Concerning the EEG/ERP data, we find a negativity that resembles a summation of the face evoke N170s in the ERP analysis and activation in the high frequency gamma band (60-70Hz) just before the time subject’s report perceiving a face. This

time-frequency analysis shows that activity seems to be cover a widely brain regions: 2D scalp spectral power has first high activity values in the occipital regions that migrate to more parieto-frontal areas. The synchronization depends on the electrode sets and the highest values appear in the 30-45Hz frequency band, before the perceptual response as well. In terms synchrony we did not find intra-hemispheric assymetries but we observed response related inter-hemispheric synchronization. We have also observed perception related patterns of ventral/dorsal synchronization.

Concerning functional neuroimaging data, we have identified both a network of areas that is involved in general decision making mechanisms and in addition, a network of regions that is more specifically related to Mooney face perceptual decision.

These areas exhibit different behaviours, according to its role on the perceptual process.

Index

Abbreviations

AC – Alternating Current
ACC - Anterior Cingulated Cortex
BOLD - Blood Oxygenation Level Dependent
CRT – Cathodic Rays Tube monitor
DLPFC – Dorsolateral Prefrontal Cortex
EEG – Electroencephalography
EOG – Electrooculogram
ERP – Event Related Potential
FFA - Fusiform Face Area
FIE – Face-inversion Effect
fMRI – functional Magnetic Resonance Imaging
FOV – Field of View
FWHM – Full width half magnification
GLM – General Linear Model
GUI – Graphical User Interface
HUC – Hospitais da Universidade de Coimbra
LOC – Lateral Occipital Complex
NSL – Number of Synchrony Lines
OF – Occipito-frontal
OFA – Occipital Face Area
OFC – Orbitofrontal Cortex
OP – Occipito-parietal
OT – Occipito-temporal
PLV – Phase-locking Value
PPA – Parahipocampal Place Area
PT – Parieto-temporal
RAM – Random Access Memory
ROI – Region of Interest
SR – Sampling Rate
STS – Superior Temporal Sulcus
TE – Time of Echo
TR – Time of Repetition
VEOG – Vertical Electrooculogram

List of Figures and Tables

1 - Introduction

The structure of this thesis is as follows: in section 1 an introductory overview on the theory and hypotheses investigated in our work is presented; section 2 covers the methods and experimental procedures concerning both EEG and fMRI; results are discussed and summarized in sections 3 and 4; future work is addressed on section 5.

1.1 - Controversial hypotheses and theories on how the brain perceives faces and the perceptual decision making process

Almost every theory concerning the function of the brain is a potential matter for discussion. A long time ago, classical phrenologists believed that discrete brain regions were responsible for complex traits. On the other hand, modern researchers (aside from a minority of neophrenologists) recognize that a single brain region may participate in more than one function; cognitive functions being processed in distributed and overlapping neural networks. Despite these points of view, substantial evidence still supports some degree of functional specialization. For example, there is strong evidence that at least one specialized cortical network runs predominantly just one cognitive function – face perception [2].

Assuming the importance of face perception in our daily lives, and that strong cognitive demands may put evolutionary pressure to functional specialization, this face-specific hypothesis would seem to be correct. However, it remains strongly controversial and many researchers argue that the processing mechanisms engaged by faces are not specific for a particular stimulus class (i.e. faces) but for a particular process [2]. This process could then run across multiple stimulus classes.

We are all experts at recognizing faces, and if we had similar expertise discriminating exemplars of a non-face category, then the same processing mechanisms would in principle be engaged. For faces we may decide on the spot which face it is (quickly processing down to subordinate classes) but for cars we may extract only the general category [2]. Few studies report that “face-like” processing of novel stimuli can be reached with just 10 hours of laboratory training [3]. Based on this type of evidence, one could argue that face-like processing can in principle emerge for most object

categories. Even so, the face-specificity hypothesis is favoured over the domain-general alternative theory [2].

It is also important to take in account that holistic/configural processing strategies may dominate in face perception, in comparison to part-based analysis. In line with this account is recent evidence suggesting that *"the probability of correctly identifying a whole face is greater than the sum of the probabilities of matching each of its component face halves"* [2]. Faces may be thereby processed as wholes rather than in a piecemeal manner, which would imply that its parts would be processed independently. Nevertheless, for inverted faces and non-face objects different pattern is often observed, indicating that this style of processing is specific to upright faces [4].

People with acquired prosopagnosia lose the ability to recognize faces after brain damage but have otherwise apparently normal object recognition. This suggests that cortical regions that are required for face recognition are not needed for object recognition [2]. This adds neurological evidence to the specificity of face processing.

Accordingly, a region in the fusiform gyrus has been related to face processing [2]. It is not only responsive to face stimuli, but is nevertheless selectively activated by faces compared with various control stimuli like objects, places or scramble objects [2, 4]. Many studies mention a consistent cluster of face-specific regions (see Figure 1) including the region of the superior temporal sulcus (STS) and occipital face area (OFA) in the occipital lobe [5]. Yet, fusiform face area (FFA) shows the most consistent and robust face-selective activation. It is located on the lateral side of the mid-fusiform gyrus and "*seems to respond generally to a wide range of features spanning the whole face*" [2]. Indeed, FFA is involved in both detection and identification of faces. Also well described is the object-selective region called lateral occipital complex (LOC) [5]. While LOC shows robust responses to inverted Mooney faces, FFA responds more strongly to upright Mooney faces than to upside down Mooney faces, especially if they are more difficult to perceive (see Figure 7(C)) [1, 2, 3]. Different behavioural and electrophysiological studies of this face inversion effect have been performed over the last decades. All recent neuroimaging studies state that inverted face perception needs the recruitment of additional areas like the ones that are house-responsive [2]. This could be the reason why these stimuli appear to be processed like non-face objects and why prosopagnosic patients show little or no impairment in inverted face perception tasks [5]. On the other hand, in tasks with objects, inversion effects are not significant [5, 7].

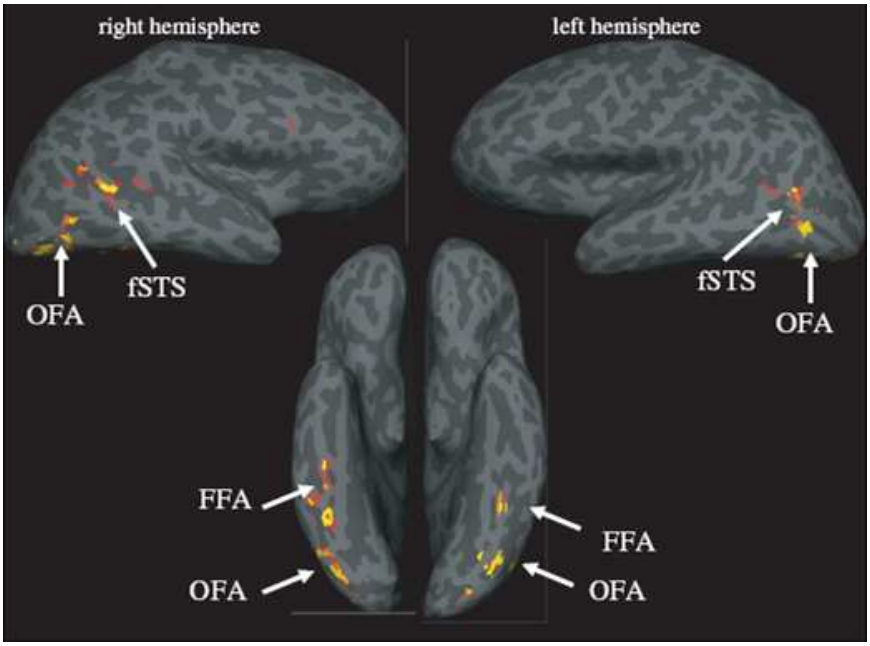

Figure 1 Face-selective activated regions (faces > objects, p<0.0001) on an inflated brain of one subject. Right and left hemispheres views (top) and ventral views (bottom). Three face specific regions are shown: FFA in the fusiform gyrus along the ventral part of the brain, the OFA in the lateral occipital area and the fSTS. Adapted from [2].

Previews Event-related Potential (ERP) studies have also been done to provide evidence of face processing in face/non-face discrimination tasks [10]. Mooney face perception was reported to be processed holistically and recognition to occur fast when stimuli are upright [8, 9, 10].

Moreover functional magnetic resonance imaging (fMRI) experiments that compared face vs. non-face processing found a close relationship between the timing of perceptual decisions about faces and the increase in top-down connectivity from frontal cortex to brain face areas [11]. This leads us to other controversial and highly debated field in the neurosciences – the neural correlates of perceptual decision making processes and their functional connectivity.

In our daily lives we are constantly deciding whether to do or not to do something. Different types of decision are possible since the decision making process involves logical analysis or circumstances of cost-benefit under certainty or uncertainty situations, respectively. Yet, in our brain many other decisions occur without our voluntary control. One could think that the choice is always ours but in fact the decision is being prepared unconsciously [12]. In fact, this could easily lead us to the

neurophilosophical discussion on the existence of free will, but this is beyond the scope of this scientific work. Nevertheless, a recent study proved that *"even several seconds before a conscious decision its outcome could be predicted from unconscious activity in the brain"* [12, 13]. Thus, different cognitive operations are involved in different types of decision making processes [14]. Decision depends also on the knowledge about physical properties of incoming stimuli and whether they are familiar or not. Unfamiliar stimuli often require intensive online cognitive processes but familiar stimuli requires a more habit-like mode of processing and respective routines [14, 15]. A variety of cognitive processes are engaged in the decision making concerning novel stimuli. Factors such as expertise, age, sex, risk or reward all impact decision making [16] and interact differently on distinct personal backgrounds. We all use our past experience in different ways depending on past experience and emotional content [16].

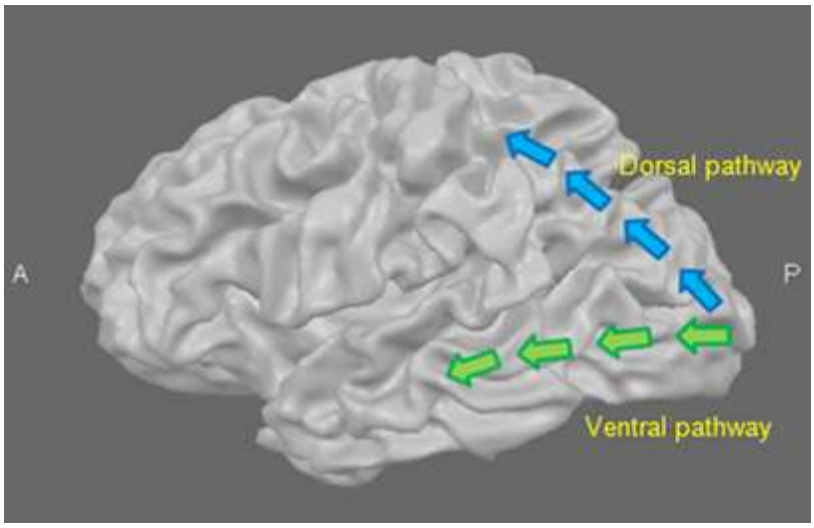

Figure 2 The ventral and dorsal stream. The two main visual pathways are shown: ventral stream connections to the temporal lobe (green) and dorsal stream connections to the parietal lobe (blue). Image adapted from BrainVoyager Brain Tutor (version 2.0, © Rainer Goebel).

Two main pathways have been described to be related with the object ("vision for recognition") and spatial processing ("vision for action") [17]. Visual information reaches the occipital lobe, is initially processed there, and flows afterwards through two main pathways – ventral (object centered) and dorsal (action centered) visual pathways (see Figure 2) [17, 18]. Ventral stream connections are mainly routed within the temporal lobe and dorsal stream project information through the parietal lobe [18]. They are associated with different functions; dorsal pathway more closely related with spatial

localization and ventral pathway plays an important role on object recognition and identification [17, 18].

Based on this, several studies were performed to identify which brain areas are involved in object processing and decision making process. The important role of anterior cingulated cortex (ACC) and orbitofrontal cortex (OFC) has been established [19, 20]. The OFC is described as underlying processing of social and emotional information and ACC would be involved in selection and control of appropriate behaviour [19, 20, 21]. These two areas act in concert with other prefrontal areas (dorsolateral prefrontal cortex - DLPFC and posterior medial frontal cortex) to make appropriate choices during the decision making process (see Figure 3) [19, 20, 22]. Moreover, other functional connections involving fronto-parietal networks[1] and thalamo-cortical circuits are associated with decision making suggesting that it involves a comprehensive network of multiple brain regions [20, 23].

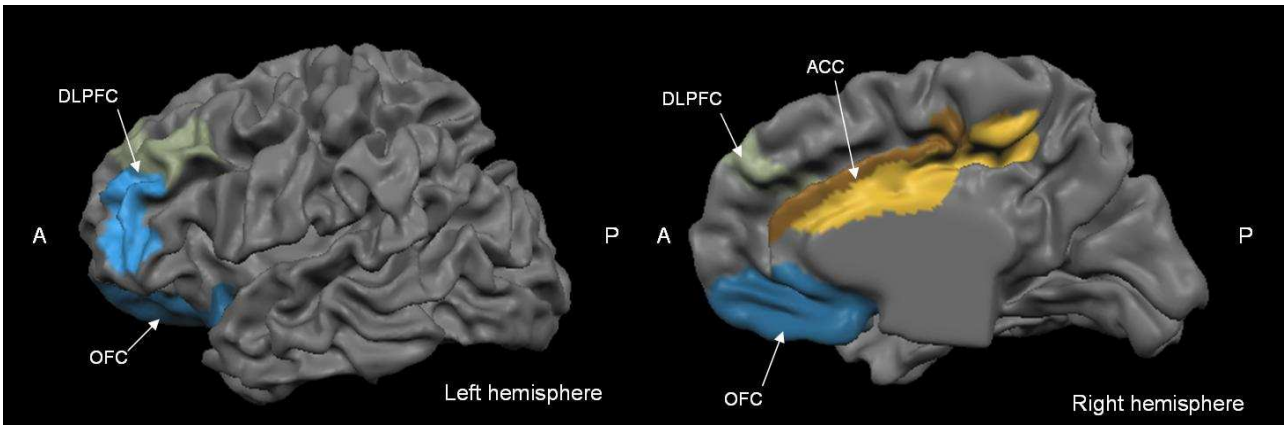

Figure 3 Brain areas with an important role in object processing and decision making processes. ACC, OFC and DLPFC are shown. Activity of these areas is, however, based upon basic cognitive capacities such as attention or working memory. Image adapted from BrainVoyager Brain Tutor (version 2.0, © Rainer Goebel).

How does the brain perform decision making? The identification of the most important brain decision-related areas were described above, but the contribution of these areas in terms of neural computations and their precise contribution to the timing of the decision remain open questions [15, 25]. However, it is already known that at least

[1] "*Fronto-parietal network have been implicated in higher-order processing such as attention, decision-making, and intelligence.*" [24]

some of these brain areas do appear have the capability to accumulate evidence about the perceptual nature of the input stimuli over time, by showing incremental changes in activity [25]. The speed and precision of the decisions are likely related to that queuing of information [25].

Despite the novel discoveries that are coming now at a fast pace, the understanding of mechanisms underlying brain function is still a tremendous challenge for the years to come. The neural correlates of decision making have been uncovered by the fMRI results reported above, but the fine dissection of the underlying processes and the many aspects that can account to the decision is a rather complex but hopefully tractable problem. Even though, researchers identified those three primary regions (OFC, ACC and DLPFC) which seem to be pivotal to human decision making as well as their connections with other different brain areas [15]. This helps us contextualize the main motivations of this work.

With this work, we aimed to understand what the role of brain face processing areas in perceptual decision making, using a Mooney face-perception task.

The general goal of this work was therefore to understand the mechanisms by which human make perceptual decisions and the specific goal to understand the role of the FFA and other ventral stream regions in this process. We sought to understand here which neural representations are activated at the moment of decision making and how that representations vary in time for different brain areas. The main questions can be summarized as follows – How does the brain perceive objects, and in particular faces? Which brain areas are necessary and/or sufficient to perceive, and decide on the categorization of different object exemplars?

All the performed work was based on two complementary imaging techniques – EEG and fMRI – with complementary spatial and temporal resolution, using a Mooney stimuli perception task.

1.2 - Electroencephalography (EEG) and Event Related Potentials (ERPs)

EEG is a technique that yields the measurement of the differences in electrical activity between different brain regions that may be cortical or subcortical [26]. The electrical activity of active nerve cells in the brain produces currents spreading through the head [26, 27]. These currents also reach the scalp surface, creating a resulting voltage on the scalp that is recorded, from electrodes placed on the scalp, as the EEG signal [27]. Indeed, EEG is the summing up of the synchronous activity of thousands of neurons with spatial radial orientation to the scalp [26, 27].

Human EEG was first recorded by the German psychiatrist Hans Berger in 1924. In the years that followed he published twenty scientific papers on the EEG field. [26, 28]

Since this historical period, many improvements have been done and in our days continuous or spontaneous EEG (i.e. the signal which can be viewed directly during recording [27, 28], without a task being necessarily performed) become an important tool for clinicians in need of diagnostic applications in the fields of epilepsy and neurooncology [27]. This technique has been useful in classifying and predicting epileptic seizures, detecting abnormal brain states or classifying sleep stages [26, 27]. It has been extensively used because it is relatively cheap and easy to perform [27].

The investigation of specific perceptual or cognitive processes, e.g. the recording of event related potentials (ERPs) requires additional sophisticated data processing techniques [27]. ERP time-course results are relatively fixed at one recording site but obviously different at different recording sites on the head and are classically labelled according to their polarity and latency [27], e.g. P100 refers to a positive potential around 100ms and N170 is a negative peak with latency of 170ms, which is a characteristic component widely believed to be selective for faces [7, 8] (see Figure 4). The N170 is in general reported to be greater and/or delayed in upside-down faces [7, 29] (a finding that we have replicated, see Figure 4 for details) but a recent publication in this field did not show N170 amplitude inversion effect for Mooney faces stimuli [8].

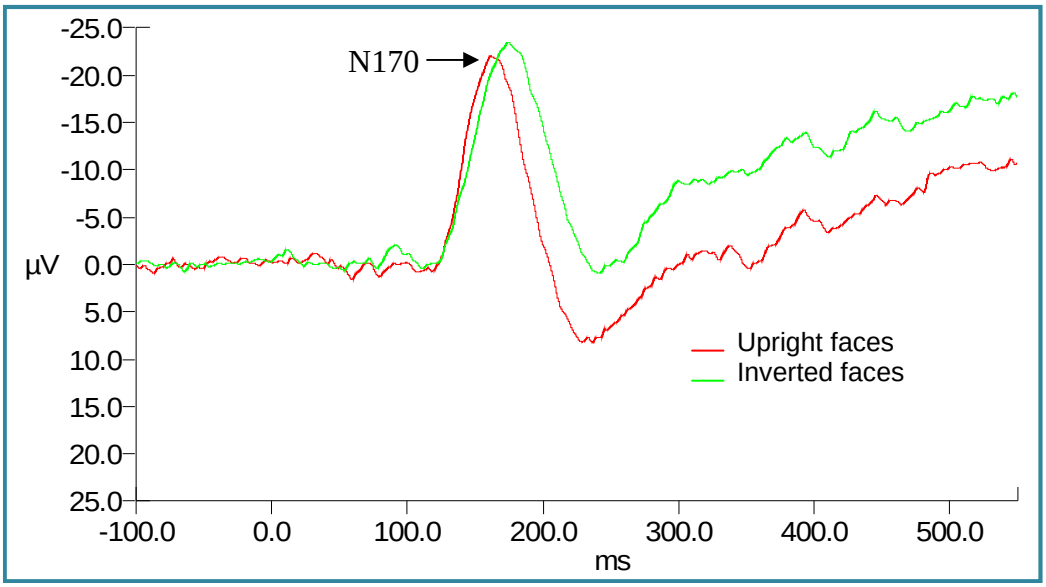

Figure 4 N170 ERP is characteristically obtained in response to faces. This chart shows the N170 peak for a representative subject in one face inversion effect experience. Results recorded and analyzed in our lab; experimental details are as follows: 30 face stimuli (15 upright and 15 inverted male/female face photographs) were shown for 300ms, and after this period subjects had a window of 2500ms to report – by means of a button press – the perceived gender (male or female) of the target image. Interstimulus interval was 3500ms. The task ensured stable attention and that subject really processed the stimuli. Red line: average response to up-right faces; green line: average response to inverted face stimuli. N170 is greater and/or delayed in upside-down faces.

Among the main neurophysiological signals that can be recorded, one can list two main types of activity: spontaneous EEG activity, evoked or also so-called event related potentials (those response components of the EEG that occur phase-locked to a stimulus[1]) [26]. These signals are in fact macrosignals, because they reflect the activity of large populations of neurons. Spatial resolution may be increase with direct electrocorticographic recording, whereby one can obtain a more localized EEG (also called local field potential) [26]. In some epilepsy patients and of course in animals one may also record single-neuron activity (using microelectrodes with appropriate impedance) [26, 27].

[1] Different stimulus types are possible – visual, electric, auditory, etc.

EEG is a non-invasive approach that can be applied repeatedly to all kind of patients[1]. EEG has virtually no risk or limitation, and its main advantage is the millisecond temporal resolution in contrast to limited spatial resolution [30]. Even with a large number of EEG recording locations around the head a non-ambiguous localisation of the activity inside the brain would not be possible [30]. This so-called inverse problem is *"comparable to reconstructing an object from its shadow: only some features (the shape) are uniquely determined, other have to be deduced"* [27]. Notice here that it is nowadays possible to record cortical EEG from grids of electrodes located on cortex or even action potential from single-neurons (using microelectrodes). These invasive strategies are useful in situations where is important to precisely identify brain areas since they improve the spatial resolution of EEG and validate localization approaches [27, 30].

The combination of EEG with fMRI is one of the latest technological developments in the field. This co-registry allies the superior spatial resolution of fMRI with the better temporal resolution of EEG.

1.2.1 - EEG gamma band activity and phase synchrony

EEG signal is composed by a combination of various waves or components – often decomposed, like any signal, through Fourier analysis. It is possible to differentiate from alpha, beta, theta, delta or gamma frequency bands. These waves are often divided in the following frequency range spectrum [30]: alpha (8-13Hz) which is probably widely studied and is related with resting and "eye closure"; beta 13-20Hz; theta 4-8Hz; delta 0.5-4Hz; gamma 20-90Hz.

The gamma band range has gained a strong focus of attention in the study of high-level brain functions [31, 32]. In recent years it has also been the arena for strong disputes and controversies. There are scientific as well as technical issues, since inadequate filtering and muscle artefacts can often compromise the data [31]. In any event, important results have been published in this field, claiming that the induced gamma band response is not an artefact but is related with cognitive processing [31, 32].

[1] We have performed EEG in normal adults. Although not in this project we could easily also perform it in children.

Synchronous activity in the gamma band has been considered to represent a central mechanism for cortical information processing [33]. Cells working in the encoding of related information, like in an object recognition task, have been hypothesized to respond simultaneously at the millisecond time scale, this synchrony representing a "tag" for the same unique object [33, 34]. This is, synchronous activity can therefore be the solution for the so-called *binding problem* in perception [34, 35]. In fact, the recognition of different object categories likely depends on distributed neural codes [35, 36]. The information about parts and properties of the object and its distinction it from other object entities is processed in a variety of brain regions, possibly requiring intra- and inter-hemispherical interactions [35]. These close and distant areas need a mechanism to "bind" the information concerning the same object, and the synchronised firing of interconnected areas is set as a candidate mechanism [33, 34, 35, 36] that is nevertheless highly controversial. Since EEG is the summation of synchronously activity of neuronal populations [26] it can be a helpful technique to elucidate the importance of large scale synchrony in brain function.

Oscillations on the gamma band are usually short (100-300ms) [33]. Even in response to identical stimuli, these oscillations are highly variable and not phase-locked to the stimulus [33]. In general, two types of activity were described: the stimulus induced oscillations (non phase-locked) and the evoked (phase-locked) activity [33].

When neural networks are activated, there is an increase of synchronized activity of many neurons in the gamma frequency band [31, 32]. This neuronal activity has been linked to different processes or cognitive functions [36, 37]. Selective attention, perceptual binding, and working memory have been highlighted as cognitive processes where gamma band synchrony is relevant [37, 38]. Furthermore, it has been associated with object representation [38] and some synchronization studies have already reported that this pattern of synchronization may also be induced by face perception [32].

1.2.2 - EEG recordings – General methodological aspects

Herewith we provide some important concepts and definitions. Recordings are taken simultaneously at all electrode locations (in our case 64 independent channels). Sampling interval is defined has the time difference between sampling points. Sampling rate (SR) is given by the number of samples per second. The experimental decision concerning choice of sample intervals depend on the purpose of the study: if the signal

of interest to be recorded contains high frequency components then a higher SR is required. On the other hand, if only low frequency components are of interest, the SR can be reduced. In typical event-related studies, a SR of 200-500Hz is enough [27].

For EEG recording a “reference electrode” has to be selected because electric potentials are only defined with respect to a reference, i.e. an arbitrarily chosen “zero level” [27, 39, 40]. The choice of the reference may differ depending on the purpose of the recording (it can be physical or recomputed to a virtual reference). The reference should theoretically not pick up signals which are not intended to be recorded, such as heart activity, which would be "subtracted in" by the referencing procedure [27]. In most studies, a reference on the head but at some distance from the other recording electrodes is chosen. Such a reference can be the ear-lobes, the nose, or the mastoids (i.e. the bone behind the ears) [40]. As stated above, it is always possible to re-reference the data to any of the recording electrodes (or linear combinations of them, like their average). In “average referencing”, one subtracts the average over all electrodes from each electrodes for each point of the time series [27, 39, 40].

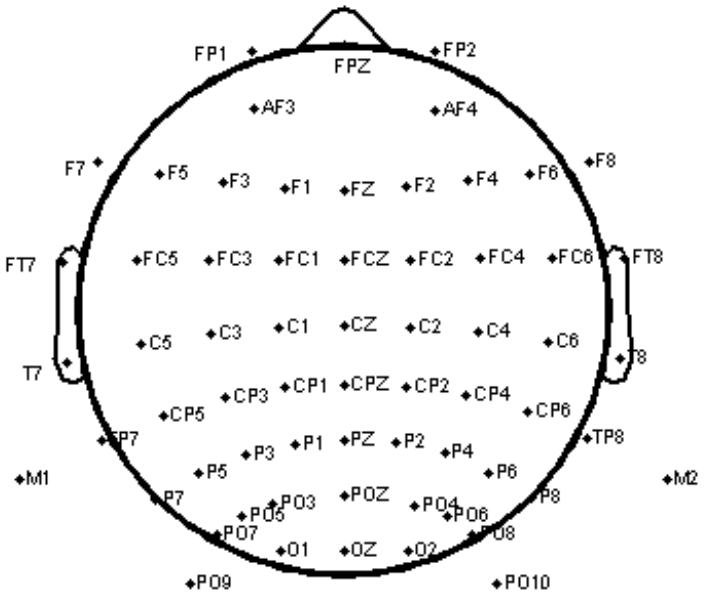

Figure 5 Channel locations - 64 electrodes locations shown. Electrode locations are projected from 3D to 2D and plotted according to the international 10/20 System of electrode placement adapted to this number of electrodes. Electrodes are labelled with letters identifying the lobe and numbers to identify the hemispheric locations.

The precise electrode location is not a critical point of the recordings but to compare results over different studies and subjects, electrode locations must be standardised (see Figure 5). A common positioning system is the international 10/20 system of electrode placement (American EEG Society Guidelines, 1994), where electrode locations are defined with respect to fractions of the distance between nasion-inion locations (anterior - posterior) and the pre-auricular points (left-right) [27]. Even though, the relative locations of the electrodes with respect to specific brain structures can only be estimated very roughly [27]. If this is a crucial issue in terms of the experimental design, electrode locations can be then digitised [40]. This makes possible better solutions of the above mentioned inverse problem, in combination with realistic modelling of the head geometry for sophisticated source estimation, and furthermore with improved visualization of the results with respect to the individual brain geometry.

The brain response of a single event is usually too weak to be readily detected in single trial, due to typically low signal noise. The solution for this problem is averaging over many similar trials by assuming that the brain response does not considerably change its timing or spatial distribution during the experiment following a certain stimulus [27]. If this invariance can be assumed, then the data can be divided in time segments of a fixed length where the time point zero is defined as the onset of the stimulus. In other words, for a certain task, brain response is assumed to be the same or at least very similar from trial to trial. When averaging, the random fluctuations will cancel each other out (they might be positive or negative in different segments) and brain activity time-locked to the stimulus presentation will add up being visible in the average [27, 40]. Prior to setting up a study one have to consider how the noise influences the data. The noise level in the average data decreases with the square root of the number of trials [41] and cause a considerable limitation on the duration of the experiment. In our case, the event-related analysis is reported to the time of the motor response, which is the event of interest, signalling the time of perceptual decision.

Modern ERP[1] studies that intend topographic analysis often employ 32 to 256 electrodes [27]. The ERP signal reflects, with high temporal resolution, the patterns of phase-locked neuronal activity evoked by a stimulus [30]. Electrodes are commonly mounted on a cap and an electrically conducting substance introduced between skin and

[1] Event-related potential can be calculated by dividing continuous data in small epochs and averaging over all these epochs. Grand group average can also be performed by including the results of all subjects.

electrodes make the contact with the skin. Electrodes can be of different materials that do not interact electrically with the scalp: Tin (cheap but not recommended at low frequencies); Ag/AgCl (silver-silver chloride) electrodes, which are more frequently used in research since are proper for a larger frequency range, but Gold or Platin can also be used [27, 30]. Because the amplitude of the raw signal that is recorded is very small the montage required special amplifiers [27, 30] that amplify the signal and convert it to a digital signal. This signal can then be stored and processed on a computer.

EEG recording often requires noise removal prior to the analysis of the signal of interest [30]. To this end, post-processing filters can be applied - High pass, Low pass or Band pass filters[1]. Although depending on the purpose of the study and the signal of interest, a typical band-pass filter for the vast majority of ERP studies would be 0.1-30Hz [27]. Here we are interested on the gamma-band (20-90Hz) and the pass band of the filter has therefore to be larger, comprising a range like 15-100Hz.

Every recording is susceptible to artefacts which are undesired disturbances due by technical defects, or irrelevant biological signals (for instance deflexions due to eye blinks), or a contaminating external source of electromagnetic signals [30]. One can refer as examples, problems with electrode connectivity (loss of contact), and movements of the head or muscle activity [27]. A procedure usually called “baseline correction” is used to correct the data for some of these artefacts. It is based in a time window where one can reasonably assume that the brain is not producing any stimulus related activity [40]. For this time range, any shift from the zero line should be only due to noise sources (shifts in muscle tension or sweating could be noise sources) [27]. In most ERP studies, this "baseline interval" is defined as several milliseconds preceding the stimulus [27, 39, 40]. For each recording electrode, the averaged signal over this period is computed, and subtracted from the signal at all time points [40].

[1] High pass filter is a filter where low frequencies are removed from the signal. Low pass filters let pass only the frequencies below a threshold frequency and Band pass filters cut frequencies out of a given frequency range.

1.3 - Functional magnetic resonance imaging (fMRI)

fMRI is a relatively recent technique but the idea behind it is not new, and actually evolved through incremental contributions of many scientists. It is very interesting to read a slightly naïve anticipation of what neuroimaging became nowadays by reading what William James wrote in 1890: *"The subject to be observed lay on a delicately balanced table which could tip downwards either at the head or the foot if the weight of either end were increased. The moment emotional or intellectual activity began in the subject, down went the balance at the head-end, in consequence of the redistribution of blood in his system…"* [42].

fMRI have been used to measure brain function and over the last decade, using the BOLD signal (Blood Oxygenation Level Dependent; see below), which is basically an hemodynamic signal that acts as a low pass filter of neural activity. In the most simplistic account, it is applied in clinical, commercial settings and research to produce activation maps showing which parts of the brain are involved in a particular mental process [42]. One should however note that such "activation maps" represent just the "tip of the iceberg", that is, only brain clusters that survive a given statistical threshold related to task execution. In most of the work presented in this thesis we will use statistical maps derived from General Linear Models (GLM) of event-related fMRI experiments (whose rationale is similar to the EEG/ERP experiments) and block design experiments (where blocks comprise many sub-events that come in succession and are not separable, and alternate with baseline blocks).

In the present study we aimed to dissect the neural correlates of perceptual decision making, using the particular paradigm of detection of Mooney (two-tone ambiguous stimuli) faces. Previous studies on Mooney stimuli have focused on comparing faces vs. non-faces, contrasting the dynamics of FFA responses for two distinct stimulus types [1]. Here we perform whole-brain and region of interest (ROI) analysis of imaging data of a Mooney face detection task by manipulating time to detection through gradual stimulus rotation from inverted to upright. In this way, we were not comparing two different stimuli, but instead two different percept (presence or not of a face) of the same stimulus.

1.3.1 – Methodological aspects of fMRI recordings

Normally atomic nuclei are randomly oriented [43]. In MRI Scanner a field about 50000 times greater than the Earth's field is applied by a very powerful magnet (clinically, 1.5 or 3 Tesla) and magnetic nuclei of atoms become aligned with the direction of the field [42, 43]. Once aligned, the little individual magnetic signals add up coherently resulting in measurable signal. In MRI it is the magnetic signal from hydrogen nuclei in water (H_2O) that is detected [42, 44]. The variations in strength of the signal make possible to discriminate between grey matter, white matter and cerebral spinal fluid in structural images of the brain (see Figure 6) [43].

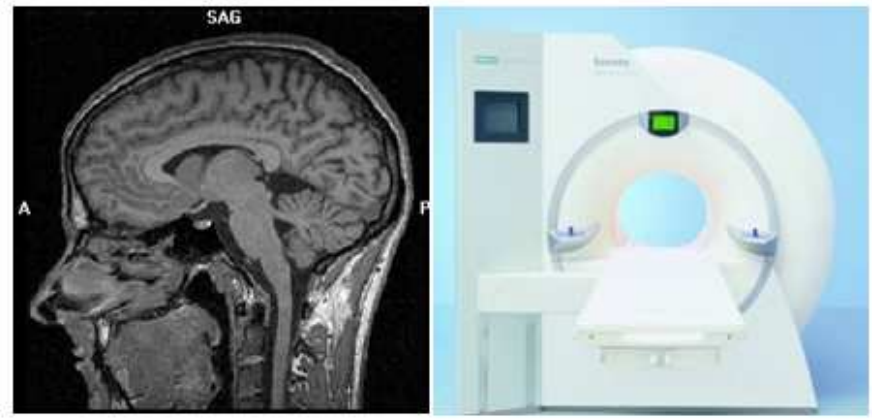

Figure 6 Anatomical image of the brain (T1 weighted). In the left is shown a sagital slice of the brain (resolution 1x1x1mm). A and P stand for anterior and posterior, respectively. Data were recorded in a Siemens Sonata 1.5T scanner (right picture; adapted from [45]).

fMRI is a standard tool for mapping statistical activation patterns in the human brain [42]. Haemoglobin carries oxygen in blood flow and has different magnetic properties (depending on being oxygenated or deoxygenated) [42, 43]. This leads to small differences of magnetic resonance signal T2* depending on the induced changes in magnetic susceptibility [42, 46]. This signal is therefore called BOLD fMRI and detects changes in blood flow (and oxygenation) that have been proved to be related to neural activity [46]. Active brain areas consume oxygen in their processes like all other cells and blood flow increases to these areas [42]. Empirically we might expect blood oxygenation to increase with activation but what happens is a momentary decrease (the

dip signal) in blood oxygenation immediately after neural activity increases (it is this signal that is usually measured) [42, 43]. This is followed by a period where blood oxygenation actually increases [42, 43, 46]. Following neural activation it reaches a peak after 6 seconds and then falls to baseline level [42, 43].

fMRI is an imaging tool with good spatial resolution (few mm^3) but temporal resolution (a few seconds) is not as good as in other techniques like EEG [42]. Since fMRI is not a direct measure of neural activity [43], and its signal act as an effective low pass filter of the underlying electrical brain activity, some criticisms are still pointed out but is still a good way to understand what is happening in the brain, as shown directly by Logothetis et al. [46].

Given the above mentioned advantages and pitfalls, some recent developments have focused on combined fMRI and EEG approaches [43]. EEG-fMRI measurements are performed simultaneously which allows the combination of the different strengths of each technique (namely the complementarities of spatial and temporal resolution). This is becoming a popular method in the field of epilepsy research and recently also in cognitive neuroscience approaches [47].

1.4 – Development of Mooney Stimuli for the perceptual decision experimental paradigm

Mooney images are two-tone degraded pictures (black and white) [9]. In general are ambiguous stimuli with little/fragmented information available to determine object content. This stimuli offer a means of inducing variable perception with constant visuo-spatial characteristics [48]. Mooney faces involve the grouping of the fragmentary parts into coherent images [9]. Craig Mooney in 1957 published the first study based on this type of stimuli [49]. He used these to test ability of children to perform a coherent perceptual impression on the basis of very little visual detail [49].

An example is shown on Figure 7. Although a face is always embedded is interesting that a first inspection to the image does not necessarily reveal the face, however, after some effort, one notices the main face features and its perceptual representation face emerges [49]. How our brain performs this perceptual task remains a debated question.

Figure 7 Examples of Mooney stimuli: (A) and (B) are two-tone upright faces and (C) is an inverted Mooney face; upside down Mooney faces are more difficult to perceive as such [50].

This type of stimuli is very useful to study perceptual decision phenomena, and it was chosen in our study since were able to manipulate the level of perceptual difficulty by adding more or less visual features, in different positions, etc. In this way we created a task where subjects were able to decide for each face if, and when, they saw it.

1.5 - Experimental design

An adequate experimental design takes critical role when trying to answer a specific question. The two main goals of experimental design are to maximize the ability to test the hypothesis and also to facilitate the generation of new hypotheses. Experimental design has to be carefully studied to get the better results. With a perfect design, controlling timing and quality of presented stimuli we can better understand and analyse resulting brain processes. To do the right approach we have to know: 1) what signals should be measured and which experimental comparisons can be adequately planned, 2) what kind of stimuli will be presented and which stimulus properties can/should be changed, 3) stimulus timing (fMRI and EEG requires different experimental protocol timing), and finally 4) the subjects task (what do subjects do during data acquisition?). [51]

One can yet differentiate between detection of regions significantly active during the perceptual task and estimation/analysis of how activity changes over time during the different perceptual epochs [51].

Different design types are possible (see also above). Block designs segregate different cognitive processes into distinct and relatively long time periods, which concatenate a series of similar events that are not separable (in other words, they cannot be discretized in the analysis). Block designs are powerful for detecting activation and useful for examining state changes but are very sensitive to signal drift (sensitive to head motion in fMRI), bad baseline choice may preclude meaningful conclusions and many tasks cannot be repeated (although this is also true to other designs). [51]

Event-related designs associate brain processes with discrete and relatively events, which may occur at any point in the scanning session. Event-related is powerful for estimating time course of activity and useful because some experimental tasks are naturally prone to be designed as event-related. However, event-related designs have disadvantages like, sensitivity to nonlinearities, which will lead to wrong estimation of underlying time courses, and difficulties determining length of “events” (except for the well defined case of length of presentation of a sensory stimulus). The main disadvantage of event-related approaches in comparison to block designs is their

reduced statistical power. Sometimes is also interesting to use a combination of these two types of design, but this makes the analysis harder. [51]

Other experimental aspects that require optimization include the facts that long stimulus presentations can lead to fatigue of subjects' attention and guessing effects are higher for very difficult stimuli; which also lead to high levels of frustration. [52]

We have thereby chosen a slow event related design.

2 - Methods

2.1 – Stimulus development and creation

Humans are particularly expert in recognizing different object categories, in particular faces. It is important to note that face appearance depends on many low and high level features like identity, facial expression, age, facial hair, face pose or illumination. It is fascinating to realize how little visual information it takes to perceive a face. Humans have evolved very effective and efficient mechanisms for the perception and recognition of faces.

To render and mask a face in a two-tone image is not easy and the creation of Mooney faces is a hard work. We have used a simple interface created on Matlab® (R2006a, The MathWorks, USA) to modify some parameters from photographs of real images to create Mooney faces. The first step was to transform real face, object and landscape photos (which were selected from various public-accessed websites) to black and white. Next, we have performed other transformations such as dilation, erosion and closure. Finally, we have made other adjustments on contrast, brightness or gamma correction, using free image processing software (PhotoFiltre 6.2.7, © António da Cruz, France). Figure 8 shows the final version of Matlab® interface.

These steps allowed for the creation of a Mooney face database that could also be used to create movies (Mooney face movies). Our Mooney movies were rotating images starting from inverted to upright. It allowed us the possibility to obtain with the same stimulus, levels of no perception or hard perception (upside-down faces) to easy perception (fully upright faces). The images are very often not perceived as faces if viewed upside down [49, 50].

240 (180 + 60) pictures in which the angle of face rotation varied in one degree step from 180º (inverted face) to 0º (upright) in the first 180 images and was kept upright in the last 60 were created in Matlab®. This *.jpeg images were converted to a 12s movie *.avi in PhotoLapse3 with a final refresh rate of 20 frames per second.

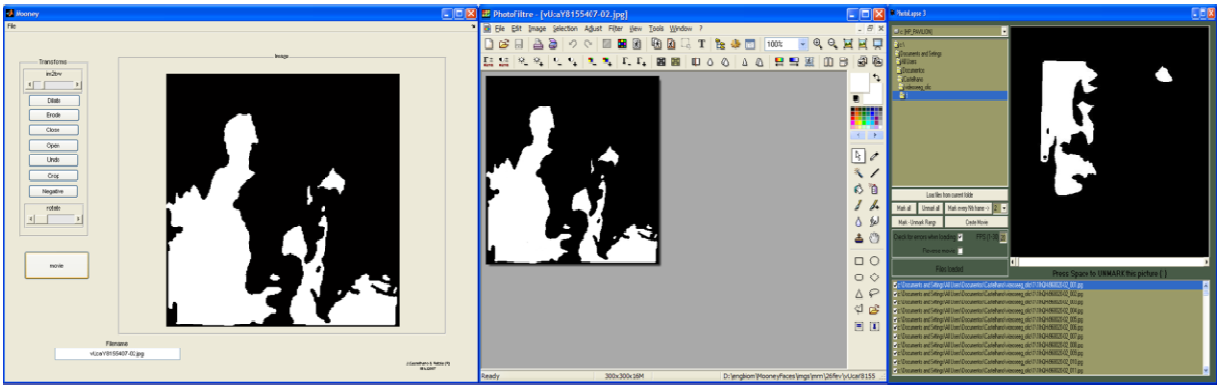

Figure 8 Custom programs for Mooney stimuli creation - from real photos to Mooney face movies. The left panel depicts the Matlab® interface used in transformations of real images to black and white two-tone pictures. In the middle is shown the Photofiltre GUI, a useful tool in this process of creating Mooney stimuli. Finally, the right panel depicts the PhotoLapse3 GUI used to convert *.jpeg images to *.avi – Mooney movies.

In the initial pilot tests we did (2 subjects in fMRI and 1 in EEG) besides Mooney movies, we did perform tests where subject had to classify stimuli in three different categories. After this step we have focused on face categories and perception of Mooney faces at different viewing angles, using a Mooney face rotating task.

2.2 - EEG experimental procedures

2.2.1 – Subjects

EEG was recorded in 11 right-handed subjects (3 males, 8 females, mean age 26.5±5.6 years). EEG recording were alternated with short breaks to avoid subject fatigue. Doing this we increase subject attention/motivation to the challenging Mooney face task. See Figure 9 with design.

All participants were either University students or scientific staff members that volunteered to participate. Most subjects (9 out of 11 subjects) were naive regarding the purpose of the study.

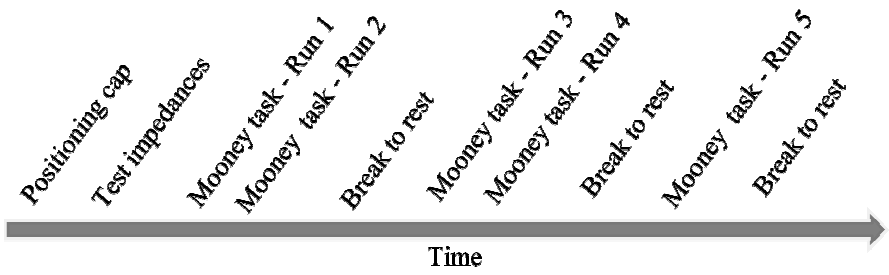

Figure 9 Time representation of recording stages/steps. Electrode impedance checking is only represented at beginning but it was also monitored along the experiment to verify recording stability. Given the long procedure of positioning the EEG cap (see below), the many recorded trials and the frequent breaks for rest, most experiments lasted about 2 hours.

2.2.2- Positioning of the EEG Cap for the 64 channel recording procedure

Materials

Before placing the cap on the scalp we checked for the availability of the following supplies:

- Quick Cap (size medium or large – 64 channels)
- Abrasive skin gel
- Tape
- Syringes
- Conductive Gel
- Alcohol
- Cotton

Positioning the Cap

Before positioning the cap we cleaned the scalp using gentle but firm back and forth motion with cotton embedded with alcohol and afterwards abrasive gel (see Figure 10(A)). For this step we gently moved across electrode location lines. It is very important that the scalp is well-cleaned during this step to guarantee good impedances and to avoid unnecessary repetitions.

Once the scalp was cleaned we positioned the cap on the subjects head. The criterion for proper localization of CZ is at the definition of the junction of the lines that go halfway between the ears and halfway between the nasion and inion. At this point, to avoid incremental discomfort, we routinely asked our subjects if cap was comfortable and without to much pressure, since the experience was quite long and to avoid the need to change to other cap size. The cap is labelled numerically and according to 10-20 system names (e.g., CZ, PO4, O2, etc).

Figure 10 Positioning the cap. (A) cleaning the scalp with alcohol and abrasive gel. (B) after positioning the cap, electrodes were filled with conductive paste using the syringe. (C) View of bipolar electrodes located around the eye to monitor eye movements. (D) Subject is seated in front of stimulation screen and prepared to participate in the experiment.

The next step was to fill each electrode with electro-gel (conductive paste to lower impedance) using a syringe and to press the electrode down with the fingers to ensure close contact with the skin (see Figure 10(B)). Using too little paste can cause poor impedances, but using too much is also an undesired risk because the paste may spread and connect two electrodes together.

A similar procedure is followed to position the electrooculogram electrodes (to monitor eye movements) and the electrocardiogram electrodes. Electrodes placed in ears' lobes and all these additional electrodes had to be fixed with tape (see Figure 10(C)).

In some subjects we have digitized electrode locations. This procedure is useful for future co-registration with data from other modalities or dipole analysis.

Testing impedances

After preparing all electrodes we connected the EEG cap to the amplifier and tested the impedances. Impedances should be as low as possible (ideally < 5KΩ). Nevertheless, depending for example on the subject hairs, it was sometimes impossible to get impedances under 5KΩ.

The acquisition hardware/software provides automatic impedance measurements and display. If the impedances were bad we had to repeat the previews preparation steps. Many times the impedances improved and stabilized during the experiment.

Acquisition setup

Prior to preparing the subject, we verified our acquisition settings (gain, filters, sampling rate, etc., see above section on EEG recording for parameters) and load this file into the acquisition system.

We explained the task to subject and the EEG data was recorded continuously for each run. Stimulation computer and acquisition computer were separate to prevent timing errors.

During the experiment we always tried to improve conditions like cable/connectors locations to prevent artefacts and minimize the noise problem.

Cleaning up

After the experiment, the cap was removed and all cleaning procedures applied (including participants scalp and cap). Normally this step was done with water running from the tap, cleaning each electrode so that no paste would remain.

Normally, two scientists/technicians participated in all stages of the experiment.

2.2.3 - Stimuli

Rotating Mooney face movies were presented at black background in a CRT monitor with resolution of 1024x768 pixels and refresh rate of 85Hz, were seen at a visual angle of ~4.5^{o}x4.5^{o}. Every stimulus appeared only once during the experiments, to prevent repetition effects.

2.2.3 – Procedure

Subjects were sit in a comfortable reclining chair in the faraday cage (darkened, acoustically treated and electrically shielded room) at a viewing distance of 120cm from the monitor presenting the stimuli.

To prevent computer RAM memory problems arising from continuous recording of data for a single large run of movies we have divided the experiment in 5 runs recorded in separate files (4 runs each one with 20 movies and a last run with 23 movies). For further processing, continuous files were then concatenated using the Append function of Edit application (version 4.3.3, Compumedics NeuroScan, USA).

All runs started with a fixation period of 10s followed by a movie face stimulus which was presented for 12 seconds (9 seconds rotating and last 3s in upright position). Stimuli were separated (inter stimulus interval) by a black screen during 3s. Short breaks were given to subjects rest between blocks.

Figure 11 Figure 11 summarizes these parameters.

Subjects were informed that all movies had a face but were instructed to respond, by pressing a button as quickly as possible, only when they were confident that they had perceived the face. Stimuli persisted after the response. All response events were recorded within the same continuous data file that contained the EEG data.

Stimuli were generated in Presentation (version 12.1, Neurobehavioral Systems, Albany) after some pilot experiments with Stim2 (version 4.0, NeuroScan, USA) which revealed lack of support to video files and potential timing problems.

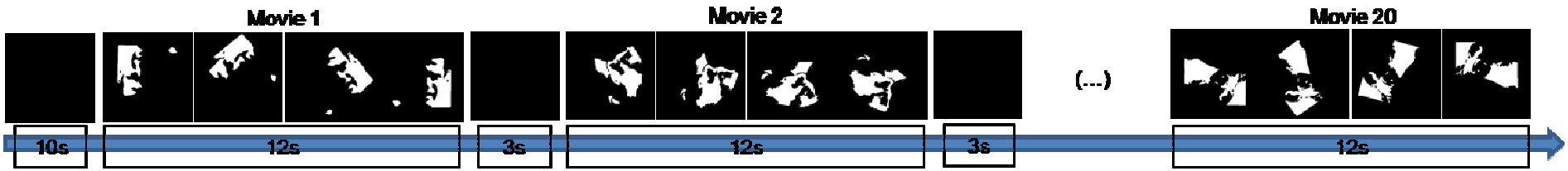

Figure 11 The time-line of one run for EEG experiments. For clarity, representative snapshots are represented in separated boxes (in the experiment movies run continuously and smoothly). Accordingly, only 4 of the total 240 frames (20Hz) are shown for each movie – faces rotate from inverted to upright in 12s movies separated by a 3s black screen. Subjects were instructed to provide a motor report, when they perceived the face, as quickly as possible.

2.2.4 - EEG Recording

We have used an electrode array of 64 Ag/AgCl electrodes (Compumedics Quick cap, NeuroScan, USA) according to the extended 10/20 system (American EEG Society Guidelines, 1994) interfaced through SynAmps2 (Compumedics NeuroScan, USA) signal amplifier, which fed the signal through the Acquire Data Acquisition software (version 4.3.1, Compumedics NeuroScan, USA) at a sampling rate (SR) of 2000Hz[1] with an active input range of ±200mV per bit and on-line low-pass of 500Hz. Gain in AC mode was set to 2010. No notch filters were used. Impedances were kept under 5kΩ. During recordings some electrodes were marked as bad and skipped from operations because of bad impedances and no reliable acquisition. Anyway, these channels were recorded.

All electrodes were referenced during recording to one reference electrode located close of CZ (for offline re-referencing, see below). The digitized EEG was saved and processed off-line.

2.2.5 - EEG analysis

The EEG was analyzed, first using Edit EEG/ERP analysis software application (version 4.3.3, Compumedics NeuroScan, USA), secondly with EEGLAB Matlab® toolbox (version 6.01b) and finally for time-frequency, synchronization and further statistical analysis with custom Matlab® functions that were kindly provided by Eugenio Rodriguez and which were adapted to work with our data.

First step on data processing was down sampling SR from 2000Hz to 500Hz. We were interested in analysing gamma-band activity so a final SR of 500Hz was satisfactory, with the added value of concomitant reduction of original file size [40].

During recordings the rule was that few channels had bad impedances. These ones were marked as bad and were rejected offline using an appropriate EEGLAB function.

[1] EEG has been recorded with a SR of 5000Hz in the initial experiments but this consumes large disk space without added benefit. Thus, with less SR (2000Hz) we reduced disk space needed to store the data and improved further processing without compromising the final analysis.

Off-line re-referencing, using average reference of all the non-rejected channels, was performed for final analysis.

The data were digitally high-pass filtered at 1Hz to remove slow drifts, using an infinite impulse response filter. To remove contamination of electrical noise, a notch-filter of 50Hz was run over all data. To perform standard ERP analysis a 1-20Hz Bandpass filter was applied. For the more advanced analysis procedures, since we were also interested in understanding modulations of gamma-band activity (20-90Hz), parallel analysis was performed by applying another Bandpass filter of 15-100Hz to the original data for further time-frequency analysis. Some authors recommend filtering continuous data, before epoching [39]. Filtering the continuous data minimizes the introduction of filtering artefacts at epoch boundaries, and we have followed these guidelines.

The Ocular artefact reduction transform function from the Edit software application (version 4.3.3, Compumedics NeuroScan, USA) was used to remove activity due to blinks. This procedure was critical because our task required some eye movements in the search for faces embedded in Mooney stimuli. These movements may contribute a lot to undesirable artefacts on EEG data which have to be corrected. Electrodes placed in the frontal and temporal regions of the scalp are more susceptible to many types of ocular artefacts. Rejecting trials that contain significant eye movements is a possibility. However, this method leads to unacceptable data loss. A more acceptable method is to "correct" the EEG based on methods that subtract a weighted fraction of an electrooculogram (EOG) from the EEG signal of particular trial.[1] Independent component analysis can also be used to perform and/or validate ocular artefact reduction.

Data were segmented into 3000ms epochs starting from -2000ms prior to response onset until 1000ms post-response onset. Some epochs were then rejected by

[1] The Ocular artefact reduction algorithm is based on the higher amplitude eye movement potentials recorded in VEOG artefact channel. Is usually used with continuous files and is important to do a review of coefficients before removing artefact to avoid introducing more artefacts.

The EOG is subtracted from the EEG channels in the following manner:

$$\text{corrected EEG} = \text{original EEG} - b*\text{EOG}$$

where b=cov(EOG/EEG)/var(EOG), b is the transmission coefficient, cov and var are the covariance and variance statistics, respectively. b is dependent of an average initiated when ocular channel exceeds 10% of the maximum estimated eye movement amplitude from VEOG.

This algorithm is good when good eye movement were recorded and for a significant number of sweeps (30 or more). [40]

visual inspection because of some other artefacts and noise (see an example in Figure 12). Baseline interval was set to -1800ms to -900ms. First point of baseline time window was not -2000ms because when one extracts epochs, a very strong discontinuity artefact at the beginning of the trial is observed. Analysis was based on these epochs' parameters after some different pilot approaches with varying time-range and test baseline periods either for response or stimuli onset. Indeed, if the baseline was too short this could lead to a wrong estimation of the variance during baseline and the normalization procedure (see below) might hence enhance non real effects.

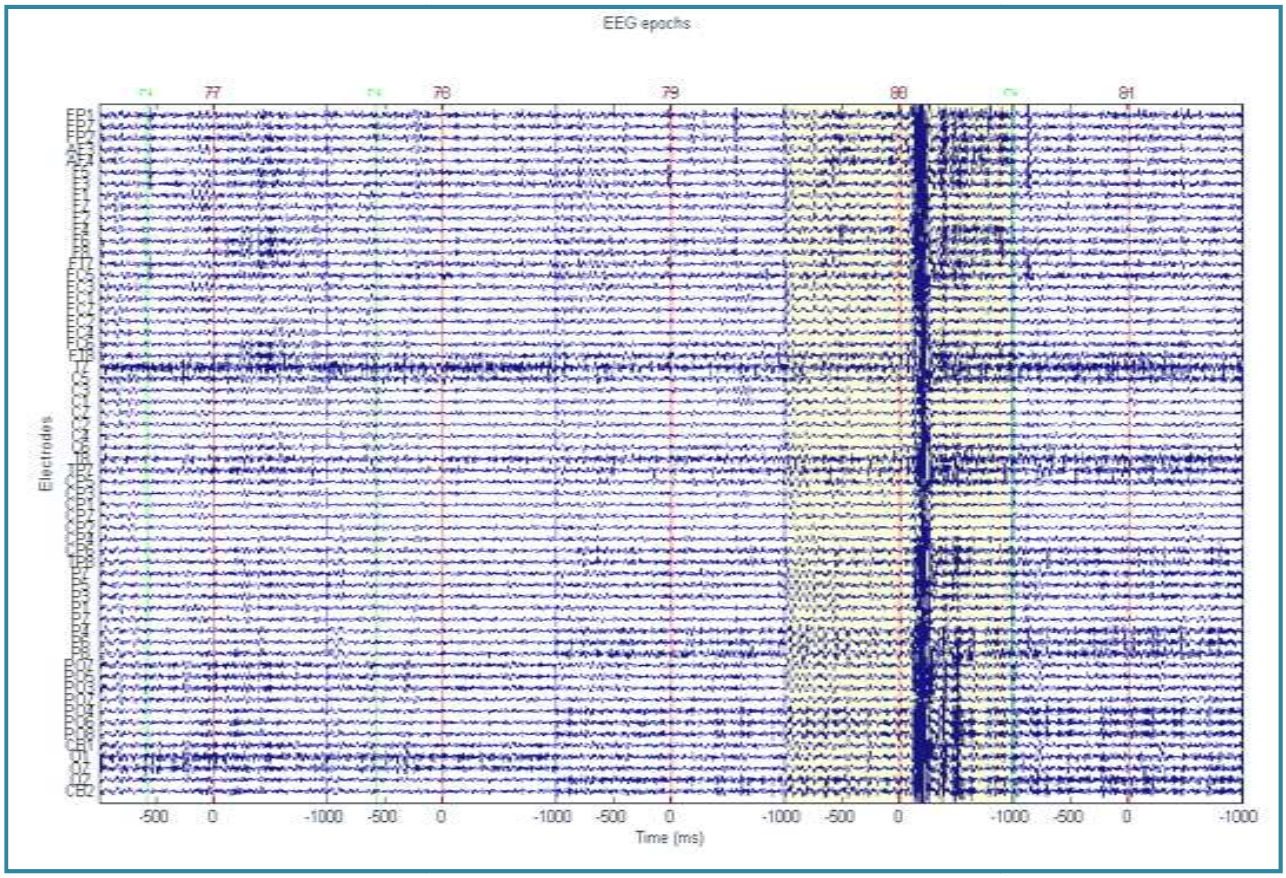

Figure 12 Data plot of distinct data epochs. In this particular case, after correction, continuous data was split into epochs of 2000ms range peri-response onset, -1000ms to 1000ms. Only 5 epochs are plotted here separated with dashed blue lines for each not rejected channel. In 3 of the 5 epochs shown are visible the stimulus event (green vertical lines) and the response event (red vertical lines) in the same second which means that subject response was very fast (faces were easily perceived). The epoch with yellow background was rejected from data because of the artefact after the response.

ERP (event-related potential)

With a time-window of -1000ms to 1000ms counting from button press (response) and to assure that all trials had the same weight, the response epochs were concatenated over subjects, and then averaged channel by channel.

Time-frequency and phase synchrony analysis

New methods are now available to separate induced and evoked activities from different frequency bands in EEG data. Averaging over sweeps is sufficient to uncover the evoked (phase-locked) activity since the random fluctuations of activity induced (non phase-locked) by stimulus will cancel each other out. On the other hand, the estimation of spectral power does not achieve discrimination between the induced and evoked activity.

Here, the estimation of evoked activity was performed by averaging over trials. The induced activity was then obtained by subtracting the evoked from the data in each trial [33].

The steps described just below were performed both for induced and induced plus evoked results patterns without major qualitative differences. The analysis was performed on single trials, and the resulting single-trial spectrograms of the absolute values were averaged.

Concerning spectral power and phase synchrony estimation:

The amplitude and phase were calculated for each time window (t) and for each frequency (f). This procedure was applied to frequencies ranging from 20Hz to 90Hz in steps of 1Hz. Considering $C(f,t)_r$ and $C(f,t)_i$ (where the subscripts stand for the real and imaginary components) the Fourier coefficients obtained for each f and t, the amplitude is given by:

$$Amp(f,t) = \sqrt{C(f,t)_r^{\,2} + C(f,t)_i^{\,2}} \quad (1)$$

This amplitude reflects the length of the vector, calculated by the theorem of Pythagoras, given by those Fourier coefficients and corresponds to the magnitude of the oscillation observed for that f and t. [48, 53]

The phase (the angle of that vector) is calculated for the same f and t:

$$\phi(f,t) = arctg\left(\frac{C(f,t)_i}{C(f,t)_r}\right) \quad (2)$$

It corresponds therefore to a point in the cycle, either peak or valley, or rising or falling slope. From this phase information is calculated the phase-locking value (PLV) that is related to neural synchrony. For certain time window is calculated the phase difference between all the pairs of electrodes and valued stability over all trials. [48, 53]

Let ϕ_i and ϕ_j the phase of the electrode signal i and j respectively. The difference in phase between them is given by:

$$\phi_{ij} = \phi_i conj(\phi_j) \qquad (3)$$

$$PLV_{ij} = abs\left(\frac{1}{N} * \sum_N \phi_{ij}\right) \qquad (4)$$

with N the number of trials. [48, 53]

For easier analysis and improved clarity of the plots, time-frequency and phase are normalized to the baseline, in this case, -1800ms to -900ms. Normalization is calculated in this way,

$$Sn = \frac{(S-\mu)}{\sigma} \qquad (5)$$

with Sn the normalized signal, S the original signal, μ and σ the average and standard deviation of the baseline[1], respectively. [48,53]

For the topographical analysis of phase synchrony (which we depict graphically by drawing lines between synchronised channels) we choose a conservative significance threshold ($p < 1e\text{-}6$). This value is based on the phase distribution of the baseline that approaches a normal distribution [48]. Thus, one line, or few lines per analysis window could be explained by chance because there are 435 (30*29/2) possible electrode combinations. Since we are using in this calculation only 30 channels, with 64 electrodes that number would be even greater.

A group average analysis was also performed. After time-frequency and phase synchrony analysis of each subject data was performed, results were averaged together across subjects, to obtain grand-averages. All the analysis was performed both for response and visual stimulus locked responses with multiple time-windows and baseline

[1] According with Rodriguez for a SR of 1kHz, a baseline time window of 500ms is well enough. Here we work with 500Hz SR and a baseline of 900ms.

periods for the occipito- parietal electrodes but also for a larger range (30 electrodes) of clusters placed all over the scalp.

In more specific post-hoc follow up analysis, comprising only between -2000ms to 1000ms from response onset epochs, the electrodes were split in anatomophysiological clusters to better understand the synchrony effects. Four electrode sets – occipito-parietal, occipito-temporal, occipito-frontal, parieto-temporal – also divided by hemisphere were defined. In Appendix A are provided the channel locations of each electrode sets.

Finally, t-tests were performed to assess significance of the observed patterns.

The analysis tree can be seen in Appendix B.

2.3 - fMRI experimental procedures

2.3.1 - Subjects

fMRI data were recorded from 15 subjects of which 10 were considered to be appropriate for further analysis (4 males, 6 females, mean age 24.7±3.5 years and one left-handed) at 1.5 Tesla (Siemens Sonata). All subjects were naive to the applied tasks and participated in the study after providing informed consent, following the approved guidelines of our Ethics Committee. All had normal or corrected to normal vision and no history of neurological problems.

2.3.2 - Stimuli

Similarly to the EEG experiments, stimuli consisted of 30 movies, each lasting 12s (see details above, in the stimulus description section). The movies showed 2-tone images of faces (Mooney faces) starting in the inverted position and slowly rotating for 9s until they reach upright position staying then fixed for 3s. Each movie contained a single embedded face and no movies were repeated. Stimuli were presented in a black background and subtended 11.5ºx11.5º of the visual field.

To map FFA, OFA, LOC and other object selective regions we have applied localizing protocols. Localizer stimuli consisted of grayscale images of faces, places (landscapes, skylines), objects (tools, cars, chairs), and scrambled versions of objects.

Stimuli were displayed on an organic LED goggle system (NNL, Norway) which allowed dioptrin correction if needed. A fibre optical signal transfer system connected the stimulation computer and the magnet room. [54]

2.3.3 - Procedure

Scans consisted of two runs of a face detection task using Mooney movie stimuli. Each run comprised 15 trials of 12s movies interleaved with 8s fixation baseline periods. Subjects were told a face was always present and instructed to respond as soon as they were confident they were seeing the face. However, it was emphasized that they should respond only when they were confident they were actually seeing the face. Free viewing was allowed.

Localizer scans consisted of two runs of alternatively viewed blocks of stimuli from a given class (faces, places, objects, scrambled images). Each run had 12 blocks and each block lasted 20s (30 images, 800ms each), separated by 10s fixation baseline intervals. During each block subjects perform a 1-to back memory task to maintain attention levels constant.

2.3.4 – fMRI data acquisition

Scanner: 1.5T Siemens Sonata (HUC, Coimbra)

Table 1 fMRI data acquisition parameters.

Parameters	Anatomical Scan	Localizer Scans	Task Scan
Sequence	T1 MPRAGE	EPI BOLD (2D) T2*	EPI BOLD (2D) T2*
Slices	128	21	21
TE	3.93ms	50ms	50ms
TR	1900ms	2000ms	2000ms
FOV	240mm	192mm	192mm
Matrix	256x256	64x64	64x64
In-plane-resolution	0.9x0.9mm	3.0x3.0mm	3.0x3.0mm
Slice Thickness	1.1mm	3.5mm	4mm
Slice Gap	0.55mm	0mm	1mm
Slice Acquisition	Ascending	Interleaved	Interleaved

2.3.5 - fMRI analysis

Data analysis

Pre-processing steps of motion correction, slice scan-time correction and linear trend removal were performed. Temporal high-pass filtering of 0.00980 Hz (3 cycles in time course) was applied as well as 3D spatial smoothing of 4mm FWHM. For all these pre-processing steps we have used BrainVoyager (Brain Innovation, Maastricht, Netherlands).

Whole-Brain group analysis

Rationale of the analysis

Our goal was to understand where and how the processes underlying face detection are implemented in the brain. We investigated which areas are involved and how their temporal patterning of activity is task related. For this purpose, we mimicked the approach explored by Ploran et al. [55] when analyzing data collected during gradual

object detection/recognition. These authors have shown that brain areas involved in decision-making tasks can be clustered into three groups characterized by their time-courses: “sensory processors”, “accumulators” and “recognition areas”. Being so, a model was built with three regressors that account for the triple dynamics of the paradigm. One of the regressors, labelled as “stimulus”, is ON during the whole period of the displayed movies. A second “decision” regressor is triggered only on the volume in which the decision was reported. A third and final “pre-decision” regressor is up for the two volumes (only in cases where there are at least two stimulus volumes before decision, i.e., only for recognition times occurring later than 4s) preceding decision. In this manner, one can identify sensory processing areas by identifying voxels with high beta values for the first regressor, recognition areas by looking for voxels with high beta values for the second regressor and accumulators by looking for voxels with high beta values for the third regressor or both second and third regressors. Although such kind of model can be argued against, it is merely a starting point. However, a network of decision-related areas consistent with recent literature [55] was found, and can be seen on Table 2.

Some of the areas are labelled just approximately, since their centers of gravity may not correspond with the ones strictly given with standard Talairach coordinates.

It can easily be seen from inspection that some areas are repeated. This is so because the ROIs are not required to exclusively belong to one of the assumed categories (“accumulators”, “sensory processors”, “recognition regions”), and the fact that statistical models will lead to partially overlapping predictors and finally also because there can actually be two or more distinct subareas within a bigger anatomically defined region. The clustering of overlapping areas is not necessarily a problem, because it can take advantage of the increased statistical power with larger numbers of voxels, etc.

After identifying the regions of interest (ROI), deconvolution analysis was performed on these areas so that the time-course of the ROI activity could be extracted. The result of this process is a curve with 10 points (activity over 10 volumes) for each event and for each area. Events were defined as: faces seen from 0-2s, from 2-4s, from 4-6s, from 6-8s, from 8-10s, from 10-12s, and unseen faces. Any partition of the

recognition times with steps below 2s would not be very informative without interpolation and other methods, since we are using a TR of 2s.

Note: since the design is slow event related (for decision periods), this procedure is similar to event related averaging since there are no overlapping predictors (concerning the decision). The magnitude can vary but not the impulse response function and consequent shape of the time-course, provided the process is linear.

Table 2 ROIs identified by GLM. Some of the areas are labelled just approximately, since their centers of gravity may not correspond with the ones strictly given with standard Talairach coordinates. r and l stand for right and left respectively.

Decision p(Bonf)<0.01	PreDecision p<0.0001	PreDecision+Decision p(Bonf)<0.0001	Other Areas of interest
l_Cingulate Gyrus	l_Caudate	l_Cingulate Gyrus 2	FFA FFX
l_Claustrum	l_Cingulate Gyrus	l_Inferior Parietal Lobule	FFA rfx
l_Culmen (Cerebellum)	l_Cuneus	l_Insula	l_amygdalaFFX
l_Inferior Parietal Lobule	l_Inferior Parietal Lobule	l_ParaCentral Lobule	maxface FFX
l_Inferior Parietal Lobule 2	l_Middle Occipital Gyrus	l_PostCentral Gyrus	MaxOface FFX
l_Insula	l_Middle Occipital Gyrus 2	l_PostCentral Gyrus 2	r_amygdala FFX
l_Lingual Gyrus	l_Middle Temporal Gyrus	l_Superior Temporal Gyrus	Stim1
l_Middle Frontal Gyrus	l_Middle Temporal Gyrus 2	r_Inferior Frontal Gyrus	Stim2
l_Middle Occipital Gyrus	l_Posterior Cingulate	r_Culmen (Cerebellum)	Stim3
l_Middle Occipital Gyrus 2	l_PreCentral Gyrus	r_Inferior Frontal Gyrus	Stim4
l_Middle Temporal Gyrus	l_PreCuneus	r_Inferior Parietal Lobule	
l_ParaCentral Lobule	l_PreCuneus 2	r_Insula	
l_PostCentral Gyrus	l_PreCuneus 3	r_Middle Frontal Gyrus	
l_PreCuneus	l_Superior Frontal Gyrus	r_PostCentral Gyrus	
l_Superior Parietal Lobule	l_Supra Marginal Gyrus	r_PreCentral Gyrus	
l_Superior Temporal Gyrus	l_Thalamus		
l_Superior Temporal Gyrus 3	r_Claustrum		
r_Culmen (Cerebellum)	r_Cuneus		
r_Culmen (Cerebellum) 2	r_Lentiform Nucleus		
r_Declive (Cerebellum)	r_Lingual Gyrus		
r_Inferior Frontal Gyrus	r_Middle Frontal Gyrus		
r_Inferior Frontal Gyrus 2	r_Middle Occipital Gyrus		
r_Inferior Parietal Lobule	r_Middle Occipital Gyrus		
r_Lentiform Nucleus	r_Middle Temporal Gyrus		
r_Lingual Gyrus	r_Middle Temporal Gyrus 2		
r_Lingual Gyrus2	r_PreCentral Gyrus		
r_Middle Frontal Gyrus 2	r_SubGyral		
r_Middle Frontal Gyrus 3	r_Superior Frontal Gyrus		
r_Middle Temporal Gyrus	r_Superior Parietal Lobule		
r_Middle Temporal Gyrus 2	r_Superior Temporal Gyrus		
r_Supra Marginal Gyrus	r_Thalamus		

Once the 7 curves were obtained for the identified areas, they were concatenated resulting in a [1x70] vector for each ROI. A 76x70 matrix containing each vector from the predefined ROIs was then formed. Other areas of interest were added to the areas in Table 2 (see last column of Table 2). These included the FFA as defined by the localizer scans (both with random effects and Fixed effects), bilateral amygdala, areas in the inferotemporal cortex that had maximum response to the stimulus in our scans (labelled Stim1 to Stim4), and areas with maximum face responses in the localizer scans (no additional contrast applied). Overall, an 86x70 matrix was available. Correlation coefficients were obtained from the relationship between each region's vector and all other vectors in the matrix. A"1-r" calculation was then performed as a means of attaining a distance measure between the regions. From these values, a dendrogram (cluster tree) depicting the region by region relationship was constructed. Dendrogram tools are included in the Statistics and Bioinformatics Toolboxes available in Matlab® (version 7.2, The MathWorks, USA).

Clustering was the next step in the analysis. However, we did not impose that all data should belong to a cluster, and we rather focused on small groups of areas with strong correlation since we were interested in grouping similar time-courses. Eight groups were defined according to the cluster tree and the rest were considered outliers.

The time courses of the grouped areas are shown in the graphs of the fMRI section of the Results and discussion chapter.

3 – Results and discussion

3.1 – EEG data

3.1.1 - Behavioural data

The behavioural data (see Table 3) revealed the challenging nature of the Mooney movie task; participants often required quite a lot of time to perceive the face (mean response time ~4.56s). Nevertheless, hit was quite high (mean ~93.64%) and we have two participants (including an absolutely naïve one) with 100% hits in all runs. However, some epochs had to be rejected (see Methods for details), as well as some bad channels, which yielded an average of ~75 epochs per subject for further analysis.

Looking closer to behavioural results we can say that face is perceived only when, at least, after rotating 90º from the inverted position[1], since subjects response time corresponds to this rotational angle. In other words, upside-down faces are intrinsically difficult to perceive and the search for Mooney faces only works when the direction of axis of image symmetry departs from fully inverted (180º).

This finding was quite consistent, despite the fact that when shown the complete set of faces (not just the ones selected for the EEG experiment) some faces were easily perceived even inverted but others were so hard that yet upright were not perceived for few subjects [50]. This self reported variability in task difficulty, as well as the scanning strategy (focusing on eyes, nose or other facial features), was very much subject dependent [49]. Future eye tracking studies may help elucidate which factors influence individual performance.

Nevertheless, for the selected stimulus set which had intermediate difficulty level, the rotational dependence was, as reported in Table 3, quite consistent. This suggest that when reaching around 90º of rotation, our stimuli can then be analysed with a mechanism that is not available for fully or partly inverted faces. We suggest that the missing mechanism is holistic/configural one, which is only available for fully/partially upright faces (or at least partially upright through mental rotation).

[1] The movie is presented at twenty frames per second and for each frame face rotate one degree to upright position (1s = rotating 20º). Time to response latency average is ~4.5s so a face needs to rotate to about 90º to be perceived.

Table 3 Summary of Behavioural Performance. Time to response is the time since movie starts till subject's button presses. The mean time to response for each run and the average of all runs is shown. Hits are the percentage of perceived faces reported. 100% would mean that all subjects see all faces in that run. Average number of channels and epochs remaining after rejection are also tabulated.

	Time to response (s)	Hits (%)	# channels	# epochs
Run 1	4.76 ± 1.49	91.88 ± 9.23	-	-
Run 2	4.88 ± 1.05	89.00 ± 10.49	-	-
Run 3	4.77 ± 1.43	94.44 ± 7.82	-	-
Run 4	3.92 ± 1.78	97.22 ± 4.25	-	-
Run 5	4.47 ± 1.23	95.65 ± 4.64	-	-
Average	**4.56 ± 0.39**	**93.64 ± 3.25**	**61 ± 2**	**75 ± 22**

Although each movie has only one face, some of the most difficult stimuli are so ambiguous that even after reporting face, subjects report that can still imagine a different face there. To visualize two faces where only one really exists is possible due to our expertise for face perception, and the constructive nature of vision, but also due to ambiguity of this stimulus. What matters for the goals of the experiment is nevertheless that they report to see a face, even if was not the one we put there. These observations do guides us to a different, but also interesting paradigm – a face imagery task that would activate the face processing networks and could still potentially be used in brain computer interface applications.

3.1.2 - Event related potential

EEG recording methodology is described already above.

Our first approach was run an ERP study where data could be split in epochs whose onset was locked to the visual stimulus or to the response. These epochs are then averaged. Here, taking account the moment of button press by the subject, the ERP analysis can show a negativity that likely reflects an expectable effect of summation of jittered N170 waves (see Figure 13). The N170 peak (characteristic for face stimulus) is not in phase, or always at the same latencies, once subject did not answer always precisely the same time after/when sees the face. Even so, the ERP show a negative curve in the -700ms to -300ms range (prior to the button press) which may well reflect

the perception of a face, after which one observes an increase around 200ms which is probably due to motor activity related to the button press. Note that we are reporting to an occipito-parietal electrode (PO6) in the figure but in the topographical maps shown (Figure 13 top), plotted for almost all recorded electrodes, the variation of activity with time and scalp location also shows this pattern.

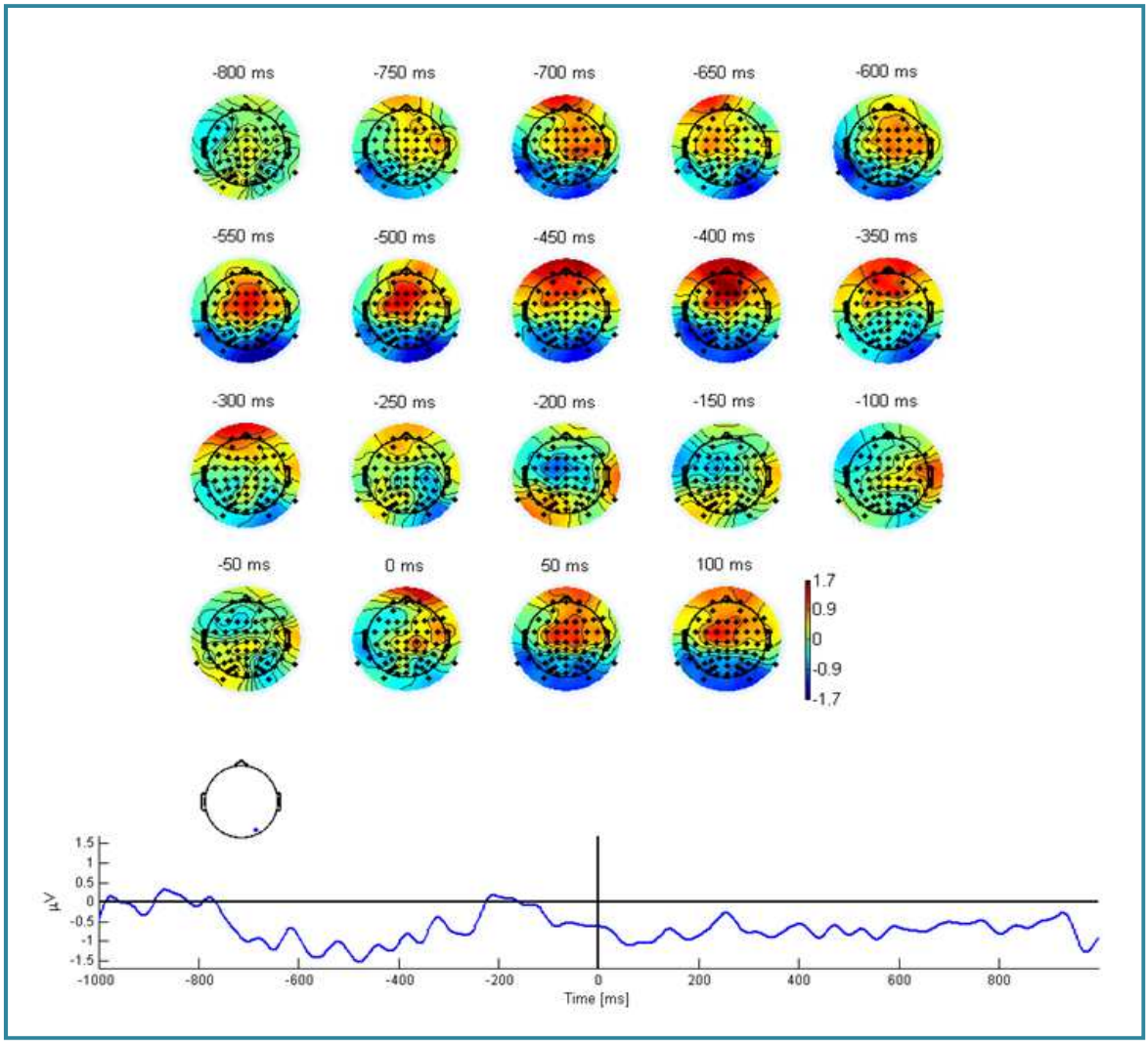

Figure 13 ERP surface maps. The top panel are the 2D maps of ERP group averages, for different time points (colorscale unit codes response amplitude in µV). Bottom plot show the ERP line for the channel PO6 (right occipito-parietal region) where N170 is often reported. 0 ms corresponds to the time of the perceptual response (button press).

One can also note a pattern of evolving frontal activity, with slightly distinct topography pre and post decision, which may reflect the recruitment of canonical decision making networks. Moreover, persisting negativity of posterior electrodes may well relate to continued reinstatement of face perception during continuous exposure to such ambiguous stimuli.

Many times the variability of phase makes the most of the components disappear in the ERP and important response components become only visible only when examining the spectral power [31]. For this reason the extended core of EEG data analysis in this study was mostly based on time-frequency and phase synchrony described before (see Methods section).

3.1.3 - Time-frequency

Our recording conditions are challenging, and even doing offline corrections artefacts such as eye movements do remain (see Figure 14). Our task needs searching for the target with the eyes, which forces special care when removing this type of artefact from our data. Figure 14 shows time-frequency and phase synchrony charts for a range of electrodes covering all scalp for induced activity. These charts are locked to the beginning of the stimulus (-1000ms to 1000ms) instead of the response onset. With the beginning of the stimulus presentation (0ms) a band in the range of 30-90Hz has the highest values. Similar types of bands have been recently described as a manifestation of miniature saccades [38]. In our case however, an eye movement explanation does not fully account for the phenomena because saccade latencies are on average 200ms [38]. This band comes earlier in time than in the Yuval-Greenberg et al. study [38], but it is sill possible that it may at least partially have the same contribution[1]. Nevertheless, since the correction and artefact rejection was rigorously performed this band must have other contributions. Furthermore, eye movements will necessarily continue due to the nature of the task, but the band is limited to the initial time of stimulus presentation. In fact, initial synchronous oscillatory gamma bursts after stimulus presentation, covering all these frequencies, have been described even in the absence of eye movements [56].

[1] Response triggers were recorded with continuous data and latencies were saved by Presentation in log files. Then the moment of the beginning of each stimulus had to be calculated from first response latency of each subject in each run.

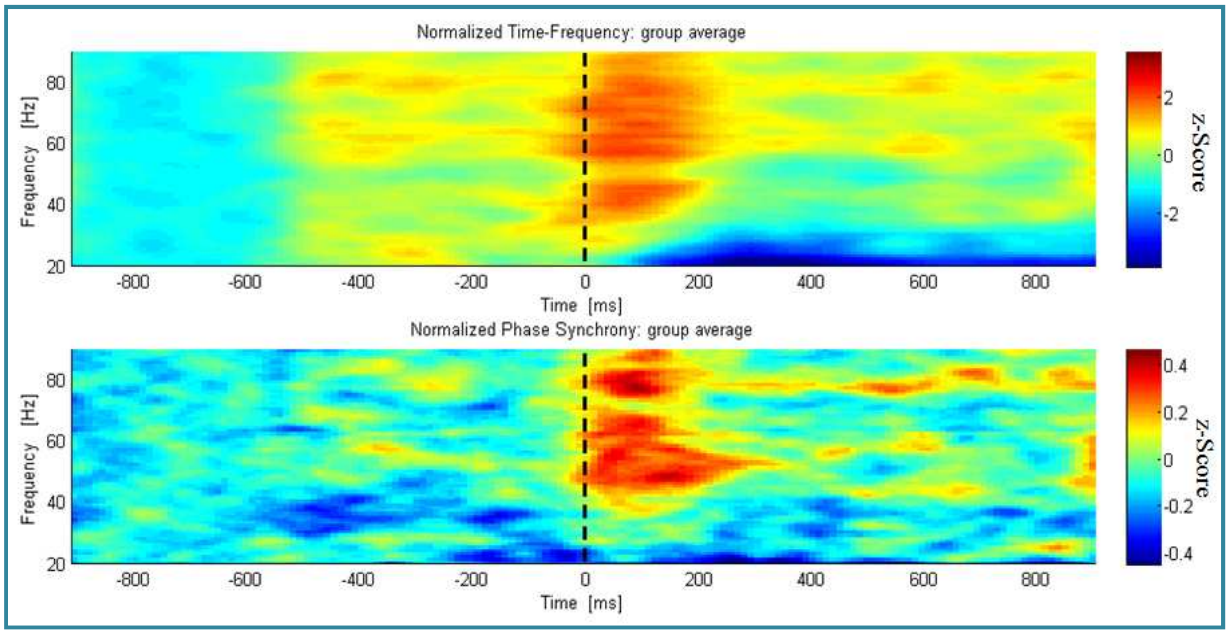

Figure 14 Initial gamma "burst" upon stimulus onset. Normalized time-frequency and normalized phase synchrony plots – stimuli onset. The black dashed line is the beginning of the stimulus. This is an average over subjects and 30 out of 60 channels from 1000ms before stimulus onset to 1000ms after it, baseline corrected for -900ms to -600ms. A strong band appears between 0-200ms either for time-frequency either for phase synchrony.

Some of the analysis options here have been established using prior pilot face processing experiments that we have performed during the last year in the Visual Neuroscience Laboratory of IBILI. One study analysed processing of emotions in morphed faces and the other the face inversion effect (delay on EEG N170 characteristic for faces, see above). These pilot experiments basically replicated findings described in the literature [29] and justify the option of focusing our analysis on occipito-parietal electrodes. These were the ones where N170 was well established so we use them for first time-frequency analysis. Results for induced activity are presented in Figure 15. In agreement with the prediction that high gamma-band have been related with cognitive processes [32], we have found increases in activity in this frequency band for electrodes located in occipito-parietal area (posterior channels), in particular at 60-70Hz. We note that these frequencies are far from the screen refreshing rate. These high values around at 60-70Hz are quite consistent and replicable regardless of the length of the baseline period used, rendering them more reliable.

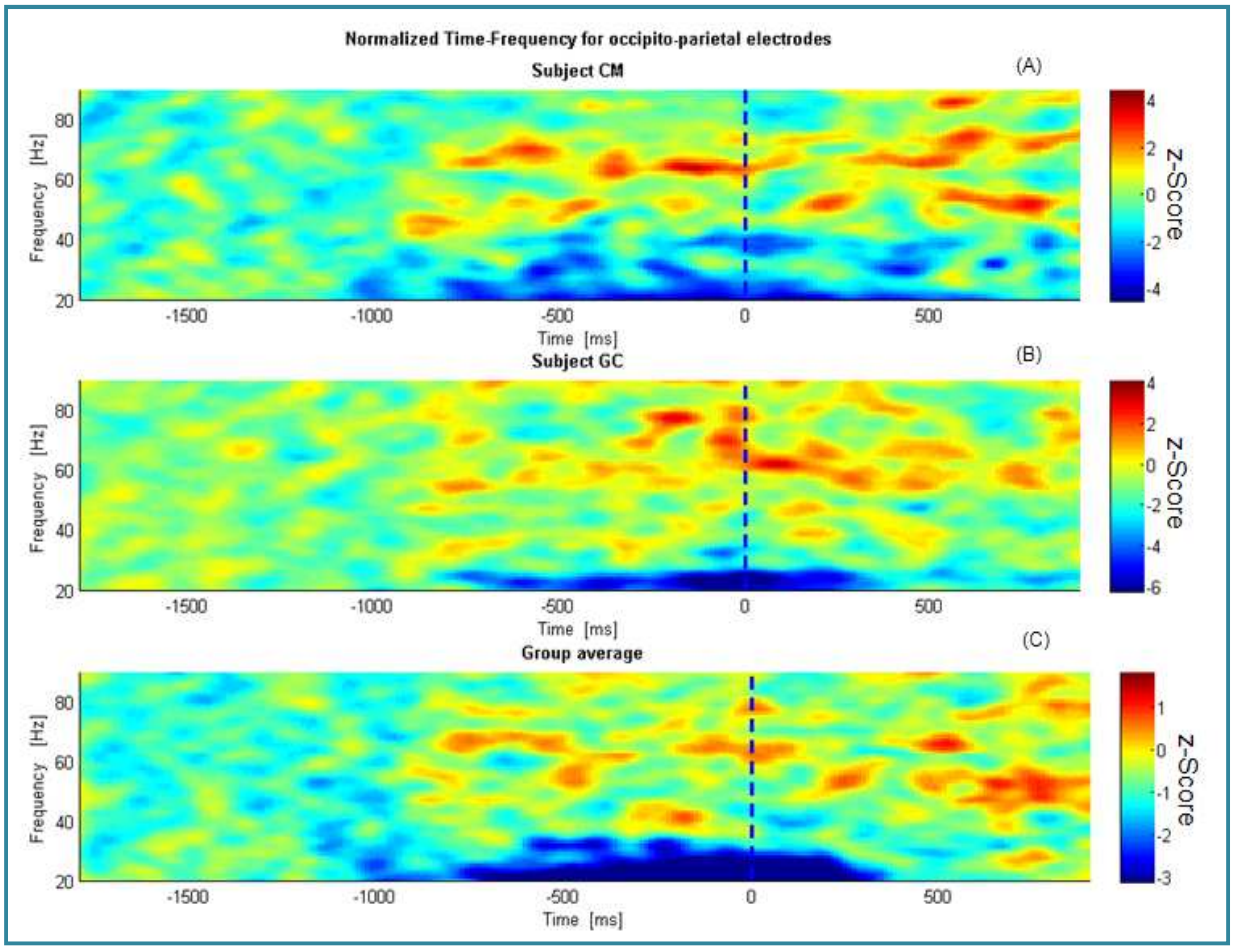

Figure 15 The time-frequency results for a cluster of fifteen posterior channels. Shown results are averages over electrodes for induced activity. (A) and (B) are results for single subjects and (C) is an average for ten subjects. Data is locked to response onset, baseline corrected for -1800ms to -900ms and normalized for the baseline interval. Higher frequency bands appears to be more prominent (~ 60Hz to 70Hz).However, higher activity is also seen before response for other frequency bands (blue dashed line represents the instant of response).

In sum for time-frequency analysis we found an interesting pattern of high gamma-band activity before response onset. As expectable from our predictions high values occurred before participants reported seeing a face. Concerning the data reported in Figure 15: the subject in (A) shows a 60Hz band is very high until few milliseconds before response (0ms) and decreases after some tens milliseconds; the subject depicted in (B), shows high gamma also present before response but also for hundreds of

milliseconds after response. The third chart (C) is a group average of ten subjects[1], and shows a pattern, that is consistent with the cases depicted in A and B, but with an emphasis that the increases occur peri-response (not exclusively before or after, but around the phenomenon of decision, and likely preceding the emergence of the percept). We did also observe a peri-response reduction in low frequency bands (horizontal blue band in the bottom of the charts) whose meaning is not clear but was a conspicuous feature of time-frequency plots.

While subjects engage in an effort to recognize the Mooney face, arousal (non-specific attention) is high. After reaching a decision, cognitive load is likely to decrease but not so for object related selective attention. Indeed selective attention to faces may even increase due to the perception of a new face. Accordingly to the literature, presenting faces should give a band around one short time window for all frequencies [32]. However, here instead of a relatively fixed vertical band, we observed a peri-response horizontal band that cannot be simply due to continuous presentation of stimuli for several seconds (otherwise should be present from the beginning and until the end). The most parsimonious explanation for this peri-response pattern is that it is tightly linked with the timing of the perceptual decision.

Assuming that the timing of brain processes is preserved across subjects (valid for the N170 components for instance), we averaged 30 electrodes (chosen to cover the whole scalp) for ten participants. Some effort was done to make a time-frequency and phase synchrony analysis including all non-rejected electrodes but this was not possible because out of memory problems. The solution was consider half electrodes each time, and then to replicate the same analysis with the other half. The results we observed for each half were very similar.

Performing a group average, the band described above is not so visible but is still clearly there (Figure 17), suggesting that although the decision related component dominates in posterior cortex, it also involves anterior regions. Activity is high in high gamma band and closely related with the upcoming report of seeing a face (response onset – blue dashed line). Results are therefore similar to the ones described before for a more restricted channel range.

[1] One subject was not included in the analysis because the reduced number of trials.

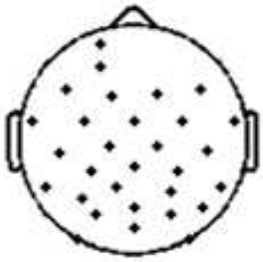

Figure 16 Channel locations. Distribution of the selected electrodes used for a more broad analysis.

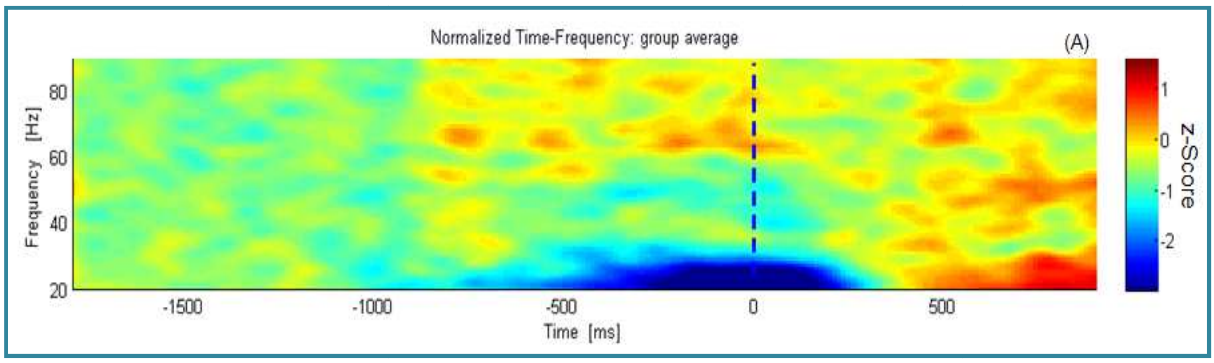

Figure 17 Time-frequency analysis of induced activity averaged for 30 electrodes over the whole scalp for ten subjects. Baseline was set to -1800ms to -900ms and the dashed blue line is the moment of response. Pre and peri-response dominance of activity in the gamma band range is still clearly visible. Note also the decrease in the low frequency band. Figure 16 illustrates the electrode locations used in the results shown here.

Plotting 2D scalp maps for the frequency band of interest and in restricted time-windows is a useful way to verify which channels provide more activation across time. It is however important that this channel based information does not refer to brain source localization per se. Nevertheless, it seems quite clear that decision related activity in that band is concentrated in occipital and parieto-frontal sites. It seems to predominate initially at occipital areas (but with concomitant anterior activations) and thereafter to more parieto-frontal regions (see Figure 18).

This recruitment of posterior and anterior areas along time can probably be related to distinct cognitive processes. Early on, frontal activity could be related to their role one decision making tasks; later on, the motor component of response will have its own contribution [57, 58].

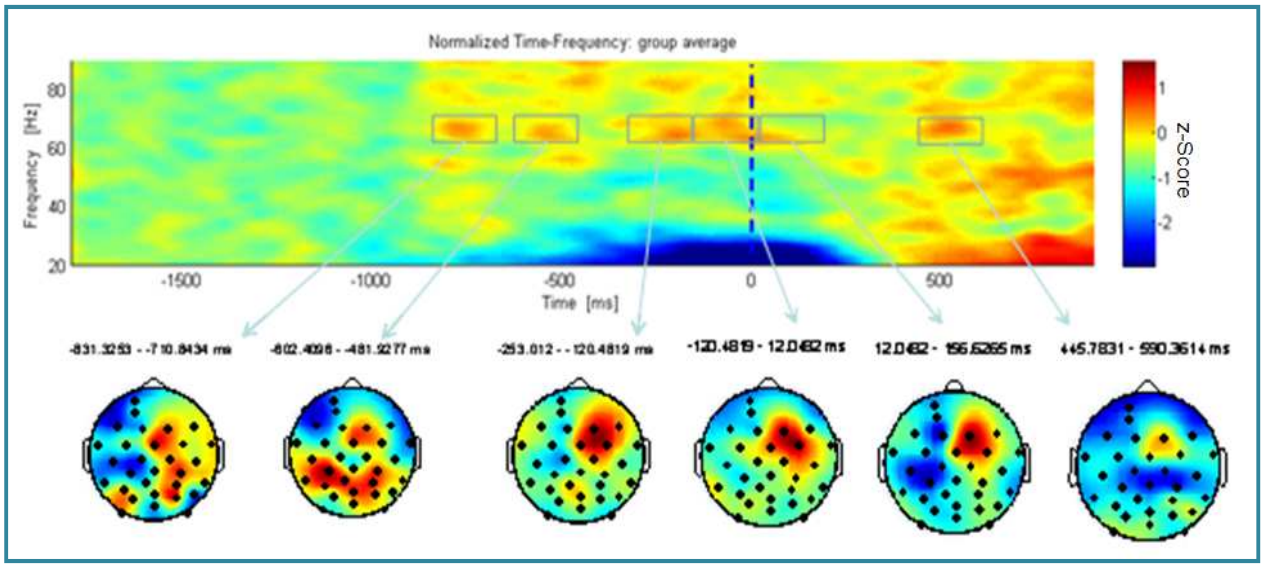

Figure 18 Normalized time-frequency plots in 2D scalp maps. 2D time-frequency (gamma power) is plotted in six consecutive time windows, for a frequency window of 62-71Hz. Each scalp plot is associated with the respective time box represented on the time-frequency plot (top panel). Notice that the 2D heads are plotted to the highest values of gamma power. Considering the six plots as whole, activity is very high not only in occipital electrodes but seems to flow during the time by the middle to more parieto-frontal areas, suggesting sensorimotor coupling. This is due to the various areas that are engaged in the sensory processing of all information we get from a face, the frontal networks related to decision and finally the motor response areas [58].

3.1.4 - Phase synchrony

Our brain is a complex structure where many processes occur simultaneously, even during a simple recognition task. The regions involved in the perception of different object categories and the decision making process, are functionally connected but the mechanism underlying such functional connectivity is still under debate. Some authors believe that the long range synchronization of neural activity plays an important role in this respect and that can to be the solution for the well known *binding problem* [35].

The analysis of phase synchrony patterns in EEG data is now starting to play an important role in this debate but its interpretation is still matter of controversy. Figure 19 shows the group average results for 30 channels. Synchronization is highly

distributed across all bands, and occurs in discrete short lived chunks. Even so, if we consider the frequency band where time-frequency have the highest values (60-70Hz) activity seems alternatively synchronised and desynchronised with time (positive values are synchronization and negative values correspond to desynchronization). On the other hand, taking the result as a whole, the synchronization is very distributed over time and frequencies, which is not surprising if one considers that one is averaging across the whole brain for online processing of complex visual material.

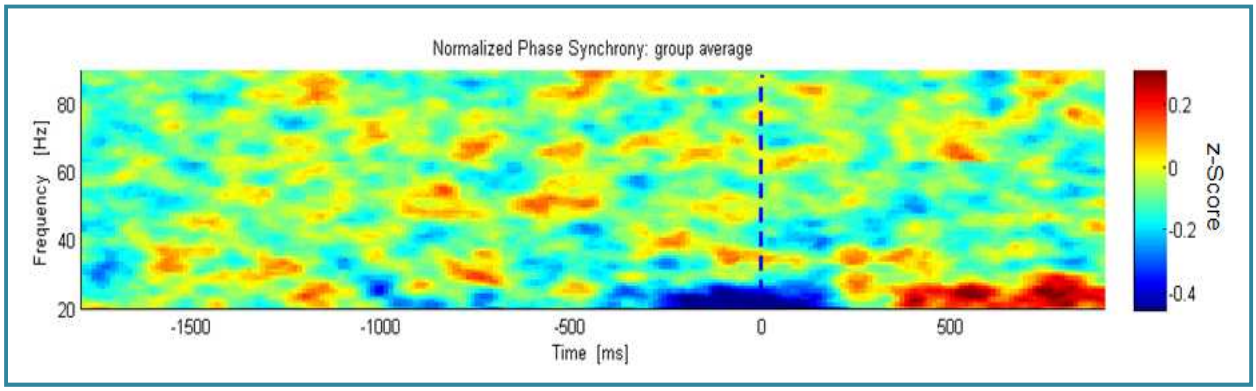

Figure 19 Phase synchrony. The synchrony was estimated for each subject for a 30 channels range covering the whole scalp, in epochs of 3000ms response locked (-2000ms to 1000ms), with a baseline time-window from -1800 to -900ms. The results were then averaged and the group average result is plotted. The blue dashed line is the button press. In the 60-70Hz frequency band, phase synchrony seems alternate their activity accordingly with the time-frequency values. These results suggest that large scale synchrony occurs in transient chunks across all frequency bands.

Averaging across many channels homogeneously distributed over the scalp may lead to blurring of effects, if they predominate in certain regions. A new analysis was therefore performed across restricted channel sets. As predicted, higher synchronization values were detected just prior to the button press and with different strength across channel sets. In Figure 20 are plotted the results for each channel set which includes both hemispheres (see Appendix A for electrode locations of each set).

An interesting pattern of frequency dependent set synchronization is observed. The occipito-frontal (OF) shows high values for multiple frequency bands, including the 60-70Hz band described above for posterior electrodes.

Interestingly, we have observed a consistent pattern of synchronization in the three other sets for the 40Hz (35 - 45Hz) frequency band. These sets have similar activation after -500ms but in the occipito-parietal (OP) set, synchronization is prolonged and with higher values. The weaker PT synchronization is consistent with the dorsal- ventral dichotomy in object processing, but a pattern of 40Hz synchrony occurring peri-decision can still be observed.

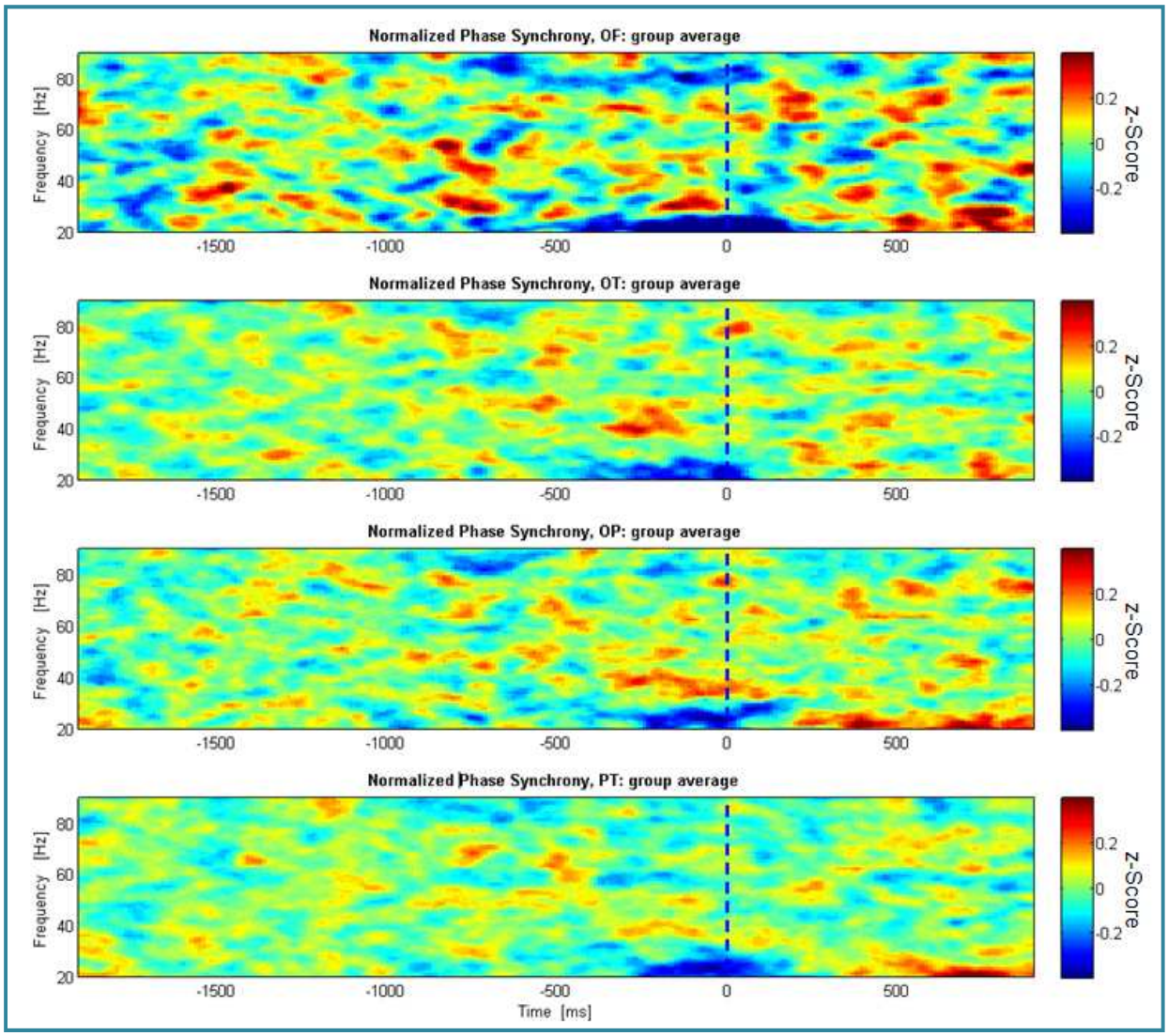

Figure 20 Phase synchrony of four different channels sets, occipito-frontal (OF), occipito-temporal (OT), occipito-parietal (OP) and parieto-temporal (PT), not divided by hemispheres. The results shown are a group average of each electrodes sets, response locked, with a baseline period of 900ms (-1800ms to -900ms). Notice the high values after -500ms around 40Hz in the OT, OP and PT plots.

Neuronal synchronization is a fast process. Considering the -500ms to 100ms (Figure 20), period, the short 40Hz occipito-temporal (OT) synchronization may be a signature of recognition within the ventral stream. OP (presumably dorsal stream) and parieto-temporal (PT, presumably dorso-ventral) synchronization patterns follow similar dynamics, suggesting the latter is a consequence of the former.

To better access the differences between electrodes sets the average of 30-45Hz band along time is plotted in Figure 21. The OF mean synchrony of that frequency band is very oscillatory, possibly reflecting the typical fluctuations of executive networks, but what is remarkable is the similar evolution of all sets pre-decision. OT, OP, PT and even OF show a concomitant increase in synchrony around -500ms. The OT (orange line) pattern is strong but short-lived (pre-decisional), in comparison to the strong OP pattern (blue line), which is peri-decisional and (to a minor degree) PT (dark blue line), which also takes more time to decrease. For that step, OP have higher values than PT and the difference between them is significant (t-test, $p<0.0001$).

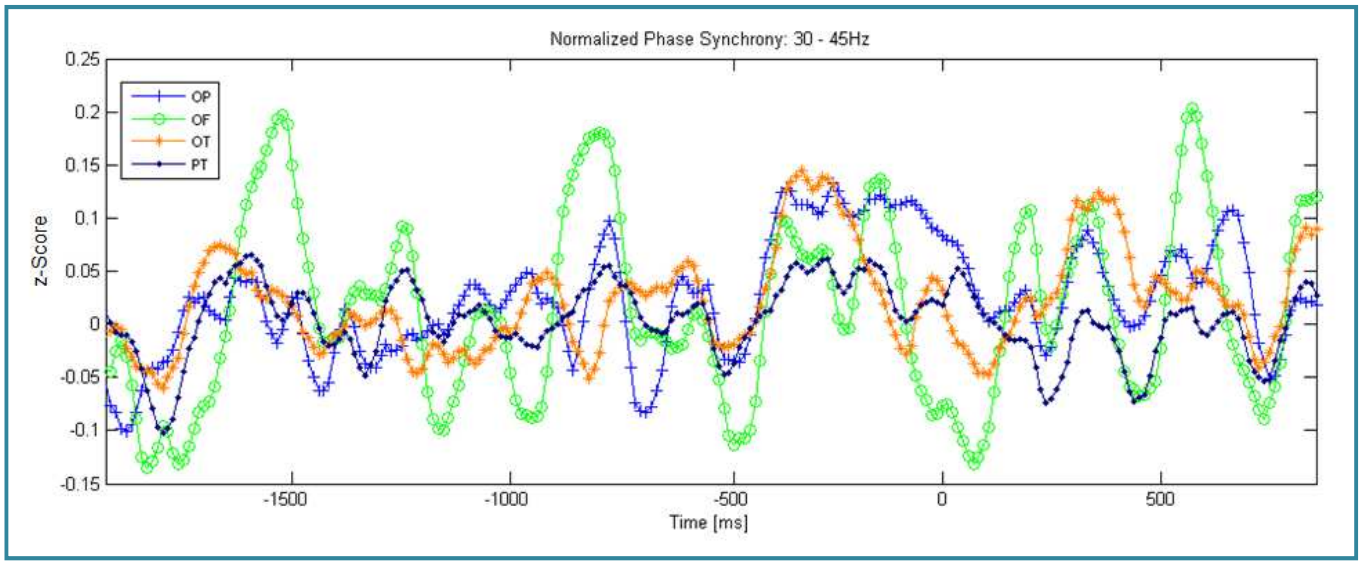

Figure 21 Phase synchrony average of 30-45Hz frequency range of the group. One line per electrodes set is representing the time evolution of the synchrony. All sets increase their activity concomitantly, 500ms prior to the decision, with a strong elevation of OP and OT above their baselines. This pattern persists for a few hundred milliseconds. It is also worth noting that OP shows a baseline fluctuating pattern that can reach high values.

Considering the PT set, the difference for the activity within the pre-decision time range -400ms to 100ms and the previews time window (-900ms to -400ms) was also significant ($p<0.0001$) what means that a different process was engaged at 40Hz, associated with the upcoming object recognition.

Since we have recorded a large number of electrodes, this leads to a large number of pair wise comparisons in the study of phase synchrony. Significant phase synchrony is highlighted by depicting topographical lines (see Figure 22). These lines connect pairs of electrodes with significant synchronization ($p<1e-6$). Notice that the number of lines is greater in the time windows corresponding to the higher values of phase synchrony. Considering the correlation across the various electrodes, the plotted synchrony lines reveal essentially the same result as shown before; synchrony beginning at OT channels (-447.2362 - -296.4824ms) than migrate to OP pairs (-296.4824 - -145.7286ms) and then evolving into a widely distributed synchronization network.

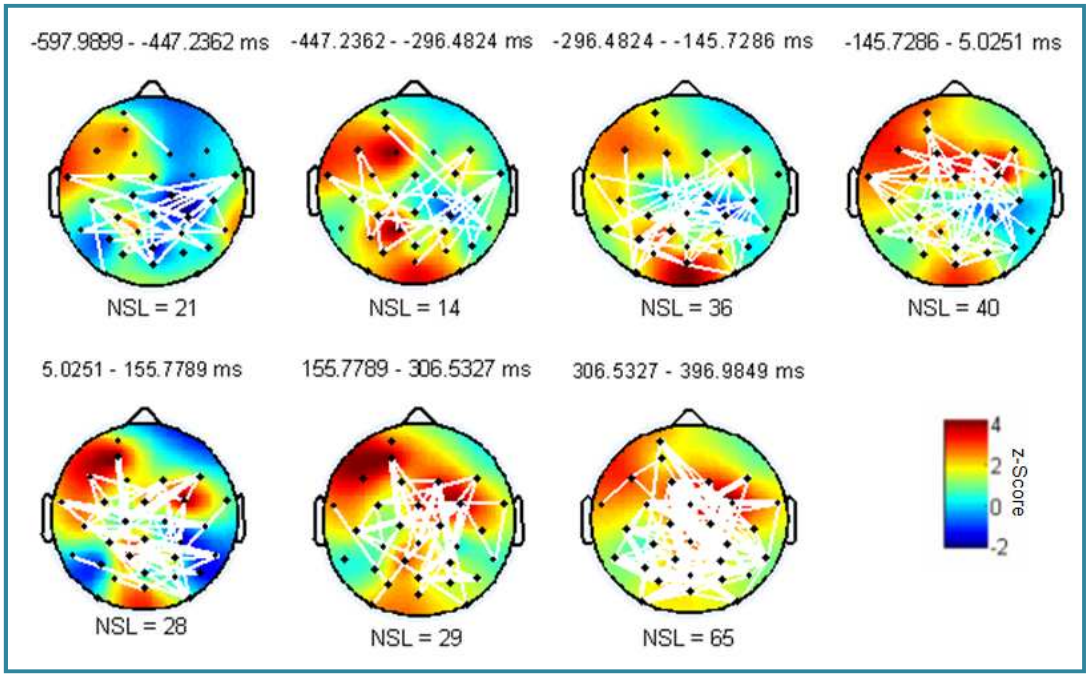

Figure 22 Group average of phase synchrony topographic maps across seven distinct epochs. Colour coding indicates gamma power average in a 33-43Hz frequency range. Significant synchrony lines connecting pairs of electrodes are displayed for each 150ms time window from -600ms response onset to +400ms in a 2D scalp map. NSL is the number of synchrony lines plotted in each head. Number of lines varies in according to the value of phase synchrony.

We have subsequently analysed the recurrence of these pair wise correlations (see Figure 23; each colour codes a given epoch, and if repeated in other epochs is again visible). A substantial number of lines are not repeated, but in any case lines in the four to seven epochs seem to be started before. Taken together, these patterns suggest that different processes occur at independent epochs (related to search, recognition and decision) and that they evolve in dynamically intertwined manner, meaning that an exchange of information occurs between activation stages.

The lines belonging to the last epoch accumulate over time, which would be consistent with an evidence accumulator model. The lines belonging to the third and fourth epoch are not present before and decrease without disappearing afterwards, with together with the time of occurrence of the third/fourth epochs suggests that they may relate to recognition. The yellow lines seem to peak upon the moment of decision report.

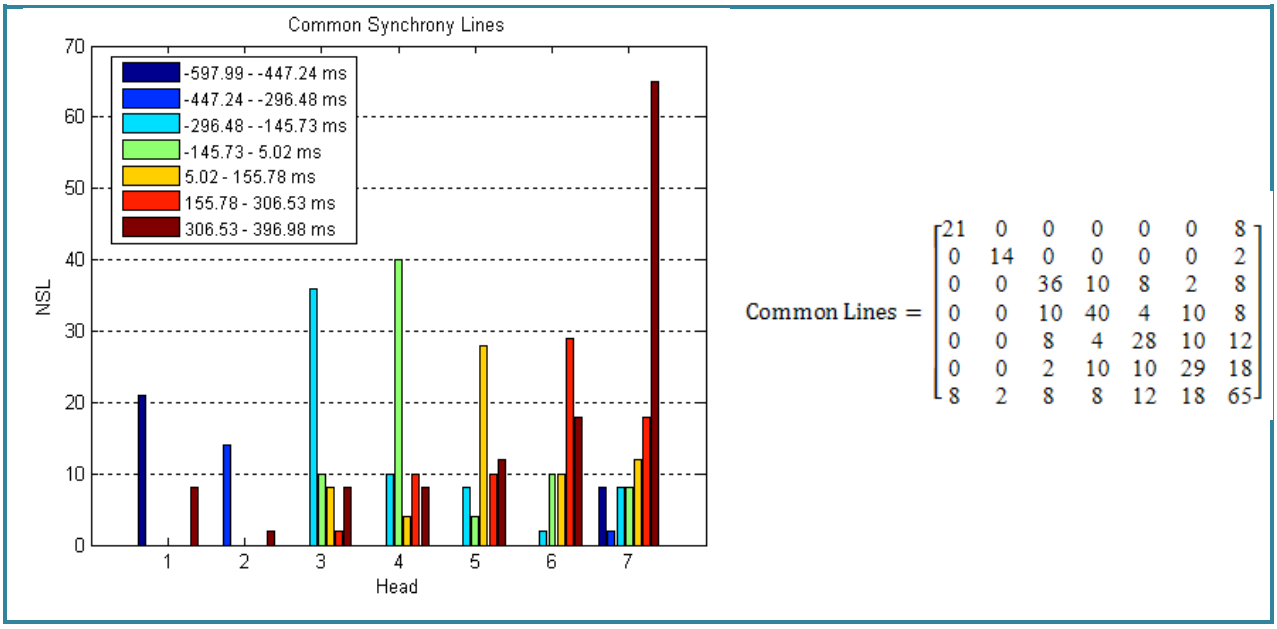

Figure 23 Phase synchrony across time as highlighted by common lines among time-windows. Each colour codes a given epoch, and if repeated in other epochs is again visible. The ones in the third epoch (baby blue) had not appeared before and are partially retained until last epoch. Most of the lines appear after this epoch, which maybe decision related. The lines in the first and second epoch, dark blue and blue respectively, only come back in the last one. The brown lines are consistent with an “evidence accumulator”. The matrix relating lines across epochs, which was used to generate the plots is at the right.

It is known that the human face processing has a right hemispheric bias [59]. To perform a hemispheric analysis, the electrode sets we have been discussing were divided by hemisphere to access the influence or the importance of each hemisphere to the phase synchrony results (Figure 24). Patterns were very similar across hemispheres and less conspicuous due to the reduced statistical power of this approach. Still, it is worth pointing out that the pre-decision 40Hz OT pattern of synchrony is still quite clearly visible, with a slight predominance in the right hemisphere. Furthermore, the highest values of synchrony in each hemisphere are at the same latencies as observed before but it seems clear that both hemispheres contribute almost equally to the global pattern of results. The two hemispheres seem to contribute equally although the inter-hemispheric connections (not considered in the intra-hemispheric analysis) can also play an important role.

This leads us to a speculating scenario where we put the inter-hemispheric connections as an important source of synchrony which seems to be corroborated by the number of topographic synchrony lines (Figure 22), crossing the hemispheres.

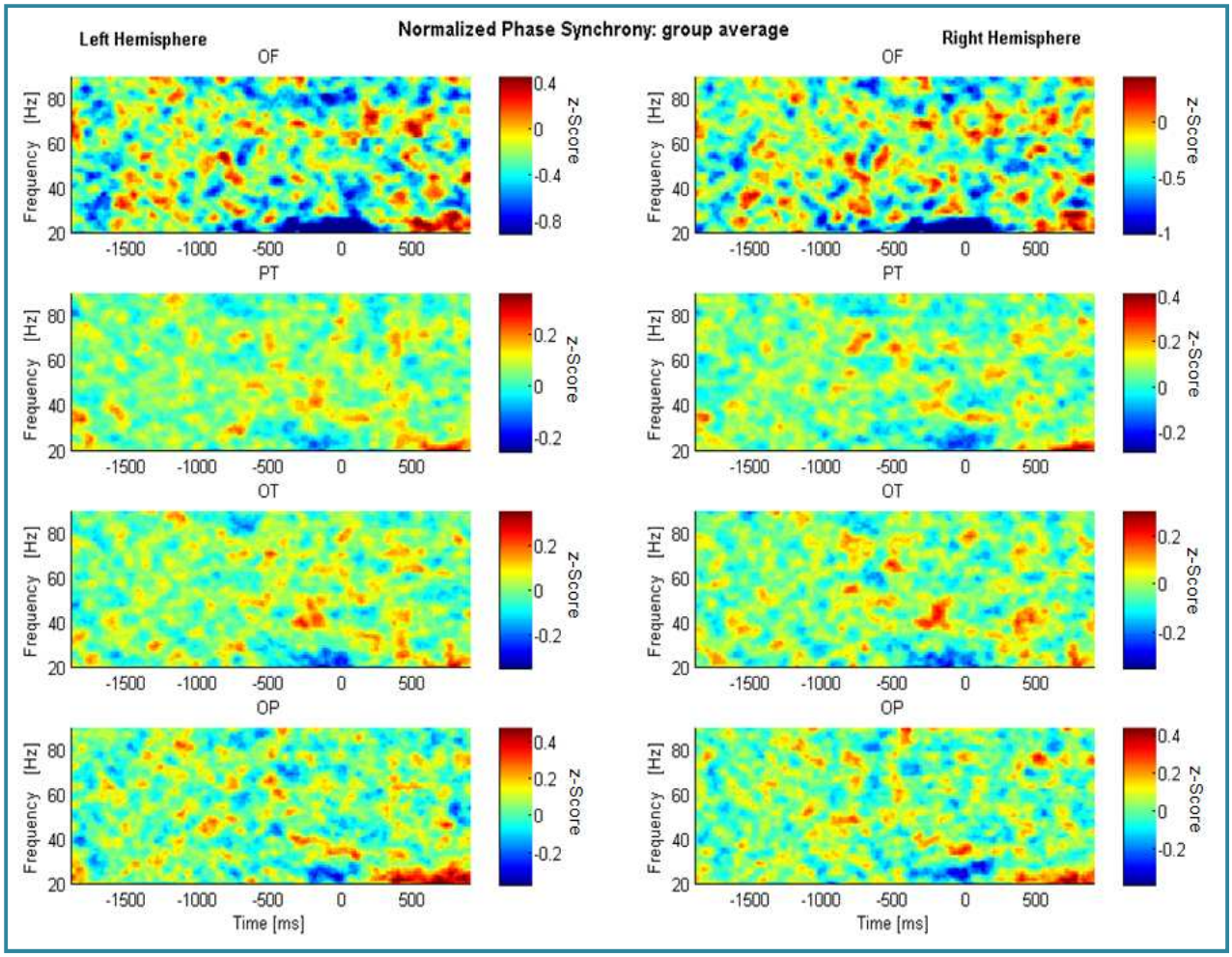

Figure 24 Phase synchrony: between hemispheres comparison. Each column refers to one hemisphere and each line to each of the electrode sets defined previously.

3.2 - fMRI data

3.2.1 - Behavioural data

During fMRI, after the two localizer runs that allowed for the identification of the brain areas involved in the perception/recognition of different categories (places, faces, houses), two runs of the Mooney rotating task were performed. Comparable to EEG, the fMRI behavioural data (Table 4) also reveals the difficulty of the task. The hit rate is even reduced (~83%) and the latencies of response are greater (~ 6.5s). This way, subjects seems to wait more than in EEG, possibly the chosen stimulus set (Mooney faces) was slightly more difficult. Indeed, recognition occurred on average around 130º rotation from upside-down for this particular experiment. The distance of the stimulation screen and effective size can account for these differences.

Table 4 The behavioural fMRI data.

	Time to response (s)	Hits (%)
Run1	6.36 ± 1.34	79.90 ± 12.01
Run2	6.59 ± 1.08	87.22 ± 9.62
Average	**6.47 ± 0.16**	**83.56 ± 5.17**

3.2.2 - Whole-Brain Group Analysis (ROIs)

The focus of our study will be to show if different patterns of activity among the identified areas can be explained by a parsimonious number of models that have already been found to be appropriate functional descriptors for other tasks [55] and thus indicate their role on the global neural circuit of face recognition processes. More specifically, as stated above, these models are: “sensory processors”, “recognition areas” and “accumulators”.

“Sensory processors”

Naturally, our brain must respond to every input stimulus it receives, making assumptions and producing decisions, even under conditions of uncertainty. Different brain regions are involved in the perception of the different object categories [60]. With the Mooney face movie task we found a set of regions in which activity is closely

related to the stimulus presence (see Table 5). Independently of the decision time, those areas show high activity during the whole time of the stimuli (see plot in Table 5), i.e., these areas are "blind" to the nature of the stimuli and only "care" about its presence. They are relay stations for higher-level visual areas and most of them have been reported as "sensory processors" [55]. They are involved in the analysis of low-level visual information contained in the movies and functionally connected with other regions which are more directly involved in deciding which kind of standard/template is similar to that input.

These areas were symmetrically distributed between hemispheres in medial and lateral regions.

Table 5 "Sensory processors". Left column: brain regions that can be modelled as "sensory processors"; numbers (in here and next tables) are arbitrary and are used to differentiate areas with similar labels. Right column: plot with the time-course in these areas (different colours represent different decision time). Independently to the time[1] of decision these areas are active for all the stimulation period.

16	l_Lingual Gyrus
17	l_Middle Occipital Gyrus
60	L_Middle Occipital Gyrus
19	l_Middle Occipital Gyrus2
61	l_Middle Occipital Gyrus2
55	l_Precuneus3
15	l_Superior Parietal Lobule
85	maxface FFX
86	MaxOface FFX
42	r_Cuneus
37	r_Lingual Gyrus
9	r_Lingual Gyrus2
34	r_Middle Occipital Gyrus
41	r_SubGyral
39	r_Superior Parietal Lobule
77	Stim1
78	Stim2
79	Stim3
80	Stim4

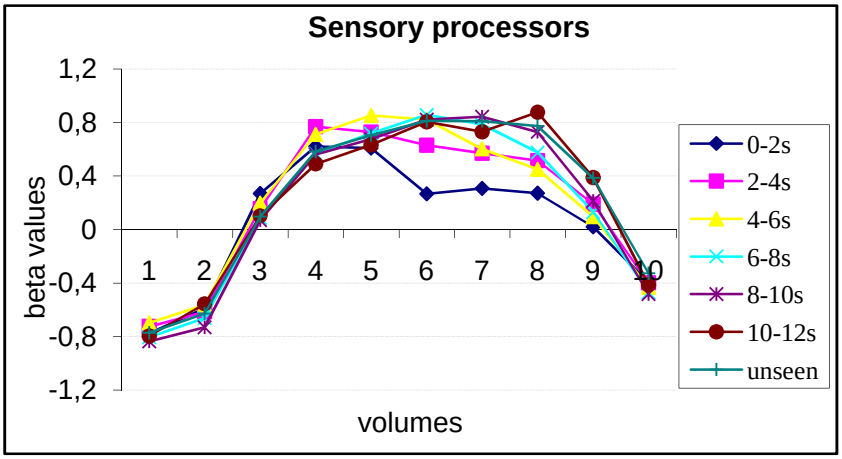

[1] Time is depicted in number of volumes (# TRs). Each volume corresponds to 2s.

"Recognition areas"

Contrary to "sensory processors", the activity of "recognition areas" tightly connects to the recognition time and not the presence of the stimulus, with abrupt rise and decay (see Figure 25). Considering the different latencies of the button press events, peaks of activity in these areas come specifically upon the moment of recognition and no peak is seen for the unseen faces (see Figure 25). These areas are thought to be high-level areas that perform perceptual decision and signal it to other areas that appropriately select behaviour given this decision. Given to its subtle variations in activity these areas have been grouped in four small clusters (see Table 6), although all of them reflect these processes. For clarity, the shown plots in Figure 25 depict the more evident cases.

Table 6 Regions labelled as "recognition areas".

Cluster 1		Cluster 2		Cluster 3		Cluster 4	
20	l_Claustrum	65	r_Inferior Frontal Gyrus	4	r_Declive (Cerebellum)	14	l_Cingulate Gyrus
27	l_Insula	30	r_Inferior Frontal Gyrus 2	64	r_Inferior Frontal Gyrus	46	l_Cingulate Gyrus
71	l_Insula	1	r_Inferior Parietal Lobule	66	r_Inferior Parietal Lobule	76	l_Cingulate Gyrus 2
25	l_PostCentral Gyrus	67	r_Middle Frontal Gyrus	29	r_Middle Frontal Gyrus 2	18	l_Inferior Parietal Lobule
72	l_PostCentral Gyrus 2	31	r_Middle Frontal Gyrus 3			75	l_ParaCentral Lobule
73	l_Superior Temporal Gyrus	3	r_Supra Marginal Gyrus			11	l_ParaCentral Lobule
26	l_Superior Temporal Gyrus 3					70	l_PostCentral Gyrus
13	r_Culmen 2					54	l_PreCentral Gyrus
28	r_Inferior Frontal Gyrus					69	r_Culmen
68	r_Insula					6	r_Culmen
62	r_PostCentral Gyrus						
63	r_PreCentral Gyrus						

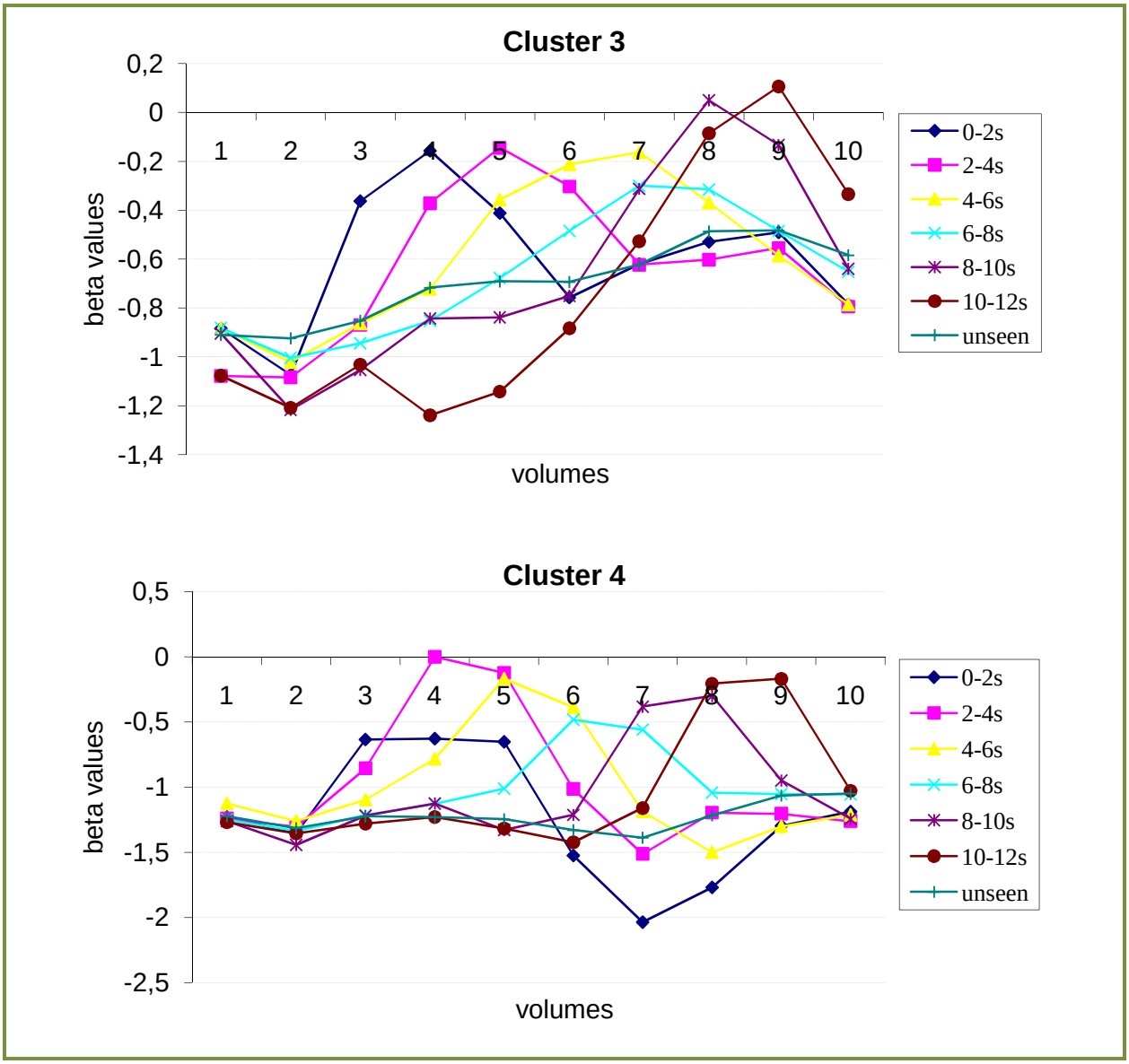

Figure 25 Time-courses for clusters 3 and 4 (see Table 6 for details) of brain regions that may be labelled as "recognition areas" (that activate around the decision). Each colour represents one different time moment (in TRs) of perceptual decision. Note that lines peaks shifts with time and no peak is seen to the unseen faces, as expected from absence of decision.

"Accumulators"

In addition to "sensory processors" and "recognition areas", there must also be intermediate processes, which progressively gather evidence until the time of decision in favour of a given outcome. In literature, the areas that carry out these processes are labelled as "accumulators" [55]. In our experiment, the left and right Thalamus and the

pre-Central Gyrus are the regions that better show such behaviour, rising incrementally before response time and behaving more smoothly. Plot depicting this activity is shown in Table 7. Furthermore, our data show that even with a TR of 2s, the causality relationship between "accumulators" and "recognition areas" can be derived from the plots, as illustrated in Figure 26 that shows that, for trials within the same recognition interval (in the depicted cases, 4-6s and 6-8s), the activity of the "accumulators" rises and peaks before the activity in "recognition areas".

Table 7 "Accumulators". Left column: brain regions whose activity patterning defines an "accumulator". Right column: plot with the time-course in these areas (different colours represent different decision time). Independently to the time of decision these areas behave smoothly presumably queuing information until the decision.

47 l_Thalamus 36 r_PreCentral Gyrus 45 r_Thalamus	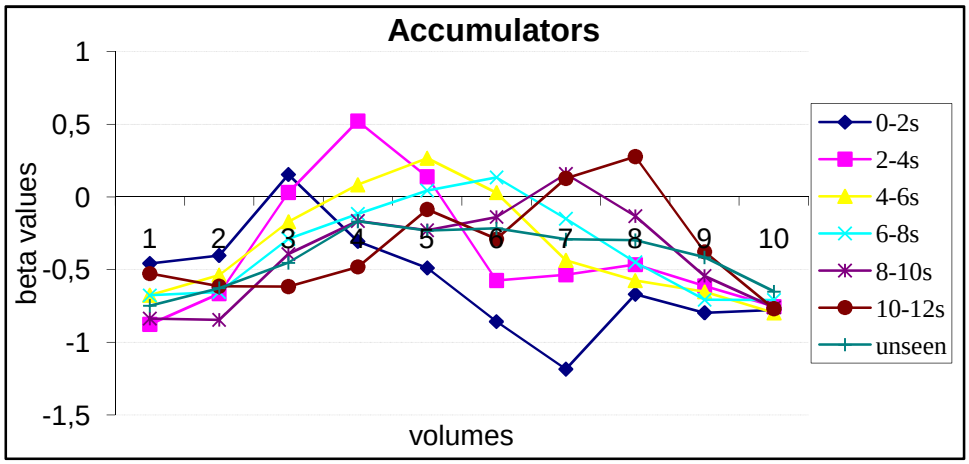

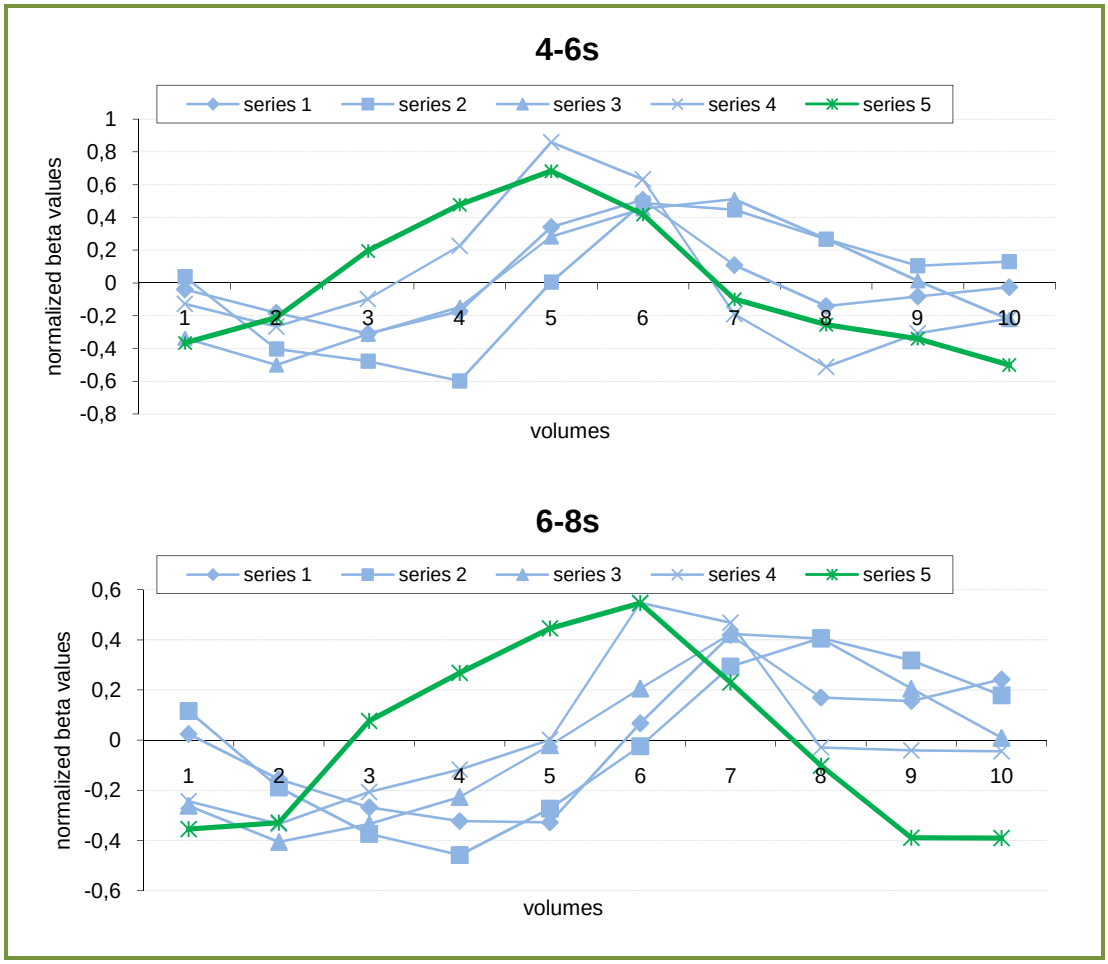

Figure 26 Comparison of time-courses of "accumulators" vs. "recognition areas" for two distinct decision moments (top: 4-6s; bottom: 6-8s). The plots depicted here show time-courses for "accumulators" (green line; brain areas: right and left thalamus and PreCentral Gyrus) and "recognition areas" (blue lines; see Table 6 for details about the regions in the different blue series/clusters). In both plots, "accumulators" rises and peaks before the activity in "recognition areas".

3.2.3 - Analysis of regions of interest specifically involved in face processing

FFA

The fusiform face area is the brain area involved in the processing of faces [2]. Oddly enough, the FFA (as identified by the localizers) does not seem to have a major role on the detection task (Figure 27). On the other hand, one area in the inferior temporal cortex bordering the FFA posteriorly and medially (Figure 28) seems to be crucial since is activated for the pre-decision and decision interval. We hypothesize that

this area is a subcluster belonging to the FFA complex. In other words, the whole of FFA is not mediating the decision. Note that the unseen epochs in this Figure 27 correspond to lower activations than other epochs, and their slightly elevated values above baseline may correspond to face expectation or imagery.

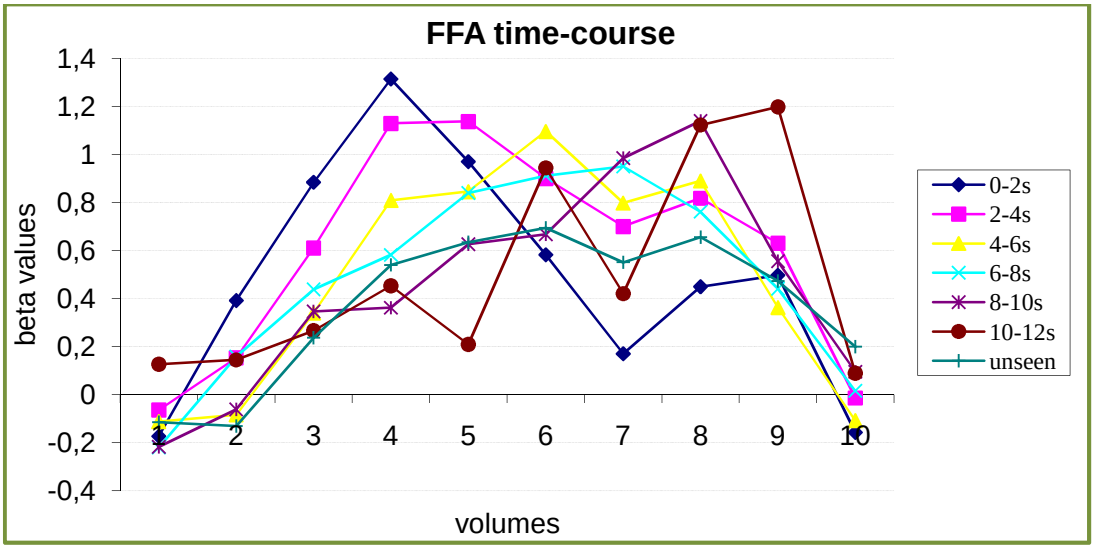

Figure 27 FFA time-course. Different lines describe different times of perceptual decision. Although unseen epochs have small values of activity than the others epochs, activity is above baseline which may be related with face expectation or imagery. FFA does not follow strictly the recognition model, but it is clearly related, at least in part to the decision.

This can lead to two conclusions. Either the localizer scans are not providing accurate localization of the FFA or there is actually a difference in face processing when the brain is dealing with ambiguous stimuli. Given the wide range of publications reporting FFA robust responses to very different face stimulus (photos, line drawings, and even smiley's) it is not easy to believe that there is a different processing area for Mooney faces. Furthermore, some of the FFA locations seem to be more anterior in the inferior temporal cortex than some previously reported locations (see Figure 28). This fact may be due to the fact that the subjects were performing a memory task (to keep attention levels constant) instead of observing passively. They were indeed performing a 1-to-back memory task during the localizer runs which may shift the location seen on other previously published contrasts. Accordingly there are for example studies claiming that face recognition is carried out more anteriorly than face detection [61]. An

independent study focusing only on the impact that a given task may have on the localizers center of gravity is currently being carried out at our lab. In any case, since the discovered area is close proximity to the FFA as defined by the functional localizer approach, we assume that it belongs to the FFA complex.

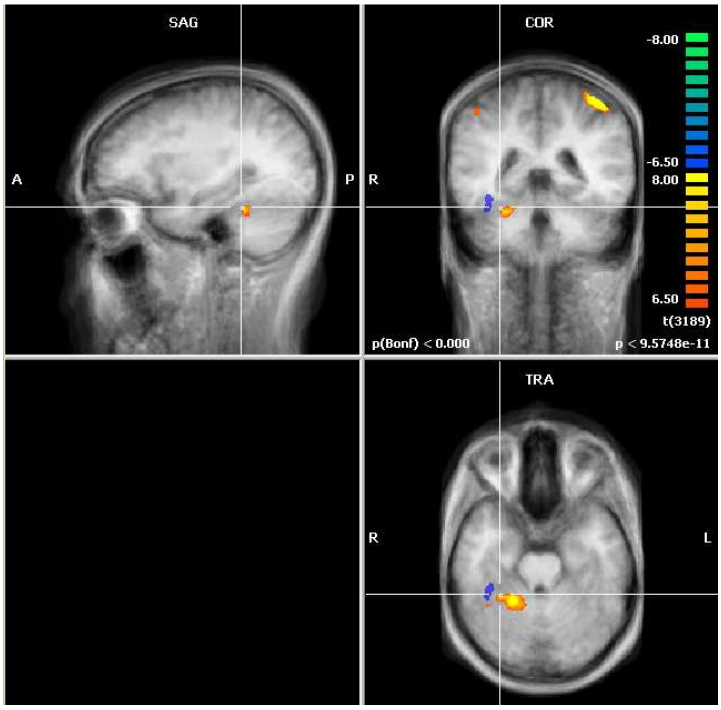

Figure 28 The blue region represents the FFA give by our localizer. The area that is active in the vicinity of FFA seems to be highly involved in the perceptual decision and recognition processes. This area is in close proximity to the FFA as defined by the functional localizer approach. We thereby assume that it belongs to the FFA complex.

On the other hand, it is also plausible that there really are some subtle differences in face processing networks when the stimuli have different properties. It has indeed been demonstrated that a large part of the inferior temporal cortex is undeniably involved in face perception tasks and Haxby et al. [62] have consistently shown that it is possible to decode which kind of stimulus is being presented just by analysing activity at high-level visual cortex, even if one masks (excludes) FFA as localized by conventional approaches. Specifically, they demonstrated that perceiving each object category was associated with a distinct spatial pattern of responses and, thus, that these patterns could be used to “decode” the perceptual or cognitive state of

the subjects [62]. These results did not change when the same analysis was performed after excluding the regions of maximal responses (e.g., after excluding the BOLD signals in the fusiform face area for the "face" category). Importantly, these findings show that information on the perceived "object category" is entailed not only in the maximally responsive or selective regions but also in a spatially wide and distributed pattern of non maximal responses in the entire ventrotemporal cortex.

Areas that deactivate during the task

We found some areas that show significant deactivation patterns around the decision events (see plot in Table 8). Some of these areas are characteristic of the well described default network [63].

Table 8 Brain regions that deactivated around time of perceptual decision. In the left column is the name of these areas and in the right column the correspondent plot (different colour lines means different time of perceptual decision). Note that activity in these areas decrease, independently of the precise time of decision.

10 l_Middle Frontal Gyrus 56 l_Middle Temporal Gyrus 51 l_Middle Temporal Gyrus 52 l_Middle Temporal Gyrus 2 33 l_Posterior Cingulate 21 l_PreCuneus 59 l_PreCuneus 44 l_Superior Frontal Gyrus 49 r_Middle Temporal Gyrus 2 24 r_Superior Frontal Gyrus	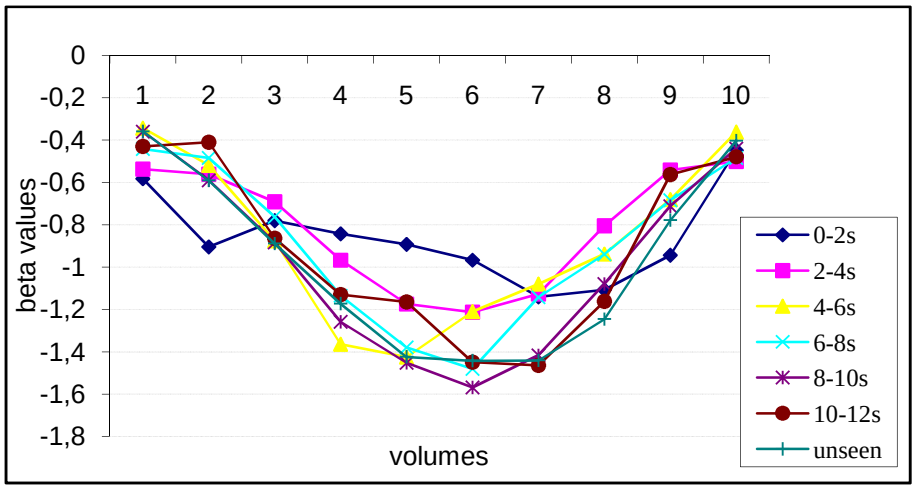

4 - Summary/conclusions

Event related potential locked to the response showed a pattern of pre-decision extended negativity, which can likely be related to summed N170 components that were jittered in time, given that the time of the exact onset of face perception also jitters in time. The negativity associated to the processing of faces that was found in our data, was precisely identified at same sites where the N170 is usually found, using the more conventional face processing protocols. Our results seem therefore to confirm that negativity at posterior sites is associated with the emergence of a face percept.

Our behavioural results also shed some light on the perceptual nature of face-plane inversion, and namely the face-inversion effect (FIE), which reflects a disproportionate difficulty in recognizing upside-down faces in comparison to other objects [64, 65]. Indeed, the fact that recognition of Mooney faces required at least a rotation of around 90º, suggests the existence of a rather fixed cut-off (the angle increasing towards upright if difficulty increase). This suggests a qualitative change in processing mode, rather than a mere gradual quantitative change. The qualitative process is a dual one: a configural/holistic-based processing mode operates for upright faces and a part-based processing mechanism is activated when faces are inverted [66]. If a dual mode exists in the plane, then one would predict a cut-off for our Mooney face paradigm where full upright (0º) and full inversion (180º) cancel out, which is at 90º. Of course this angle should increase for Mooney faces conditions where even upright stimuli are difficult to recognize. Our results match exactly these predictions.

Our Mooney faces were ideal to separate configural (implying analysis of spatial relations among facial features) and/or holistic information (whereby faces are processed as a coherent, indecomposable whole), which dominate in the upright position from piecemeal processing of face parts (e.g., isolated features such as eyes, nose, mouth) which dominate in the inverted position. This model is substantiated by some previews behavioural studies [66, 67]. This view has however remained controversial [65, 68]. Future eye-tracking studies should help to uncover the face parts observers use to discriminate faces in upright and inverted positions, and if they are the same.

Gradually rotations from upright to upside-down orientations of standard face stimuli have already been used previously to help solve this controversy. These studies have in general favoured the qualitative hypothesis by suggesting a steep decay of configural processing strategies rotation ranging from 90º to 120º rotations [69, 70, 71, 72, 73, 74]. These studies were however using standard faces which make it difficult to separate these processes cleanly. Our paradigm solved the potential use of mental rotation strategies to compensate for orientation differences. Indeed, reaction time and performance differences could merely be due to a detrimental effect of mental rotation of standard images that can already be perceived as wholes [75]. Since our Mooney stimuli could not be perceived as wholes when they were not upright, we could cleanly exclude mental rotation as an explanatory variable.

These questions have hardly been addressed in previous ERP/imaging studies. For example, it would be important to understand the role of areas commonly described as being face selective (FFA, STS and OFA) in this process. It has been hypothesized that the FFA activity does not functionally underlie holistic/configural processing of faces but rather a generic face detection system since no FIE effect was found in earlier studies [50]. However, recent studies with improved design and statistical power have shown that FFA activity modulation by face inversion exhibited a positive correlation with the behavioural FIE, unlike the other regions [76]. Our results seem to corroborate the relevance of FFA for specific face processing, thereby extending the previous results of McKeeff and Tong [1] using upright Mooney faces and Mooney non-faces. Furthermore, we do show differential activation when the same local features are present and only the perception of present/absent whole face varies. The fact that the network activated by upside-down faces is distinct from the one activated by upright stimuli also favour the duality hypothesis [77].

In our pilot ERP study of face inversion using standard faces, we have replicated the widely known latency and/or amplitude shifts of the scalp recorded occipito-temporal negative potential around 170ms (N170) [78]. Early studies have identified a positive component peaking around 160ms to 180ms over central scalp sites (Vertex Positive Potential) showing also a FIE effect [79, 80].

Our Mooney face ERP study clearly shows an occipito-temporal negativity that is associated with holistic face processing, thereby shedding some light on the debated

nature of these electrophysiological signals. Some of the previous effects, namely the increase in N170 amplitude induced by standard face inversion have been attributed to the intrinsically higher difficulty of processing inverted standard faces [7]. Our study actually directly controls for difficulty, which can be parameterized by measuring angle of recognition.

The key question of this work was however the time at which face processing takes place in the brain and its neural substrates. By showing a pre-decision negativity and no early positivity, our study seems to exclude a role for posterior positive ERP component known as P1 [81, 82], which is in agreement with a recent study that has clearly demonstrated that N170 FIE is functionally tied to the behavioural FIE [83], without any effects of rotation on P1.

We do in sum believe that our study shed some light on the debate of which ERP component reflects face processing, by identifying an fundamental discontinuity (the 90º cut-off) and the presence of a ERP negativity that was linked with the moment of recognition.

In addition to the time-locked ERP response, we have focused on the analysis of decision related patterns of activity in different frequency bands. With spectral power (time-frequency) analysis it was possible to found activity in the high gamma band described before as involved in face processing [32] and that we were now able to relate with the timing of decision making processes. The high synchrony values at 30-45Hz band, especially for the OP and OT channel sets, are the likely result of simultaneously engaged mechanisms in the dorsal and ventral stream. OT synchrony occurred quite early on a relatively short epoch, during the pre-response period, and was likely signalling the recognition, whereas OP synchrony spanned the whole peri-decision period, and was likely involved in consolidation of the decision and planning of the motor response. Synchronization is then proposed to be the mechanism of functionally connecting different brain regions both concerning the recognition, the decision process itself and the motor response.

Concerning the fMRI data, it corroborated the notion that a network of areas shows activity patterning that is closely associated with the time of decision. This network includes the left motor cortex, supplementary motor cortex, bilateral inferior frontal gyrus, parietal operculum, left insula, left thalamus, and an area on the right

inferior temporal cortex. Oddly enough, the FFA (in a restricted sense, as identified by the localizers) does not seem to have a major role on the detection task. Nevertheless, this area in the inferior temporal cortex bordering the FFA posteriorly and medially seems to be crucial to the process, and likely belongs to the FFA complex (in a broad sense).

Regarding the classification of the grouped areas in “accumulators”, “recognition areas” and/or “sensory processors”, they are in fair agreement with the one achieved by Ploran et al. [55]. This means, as expected, that the face recognition processes share the same low level core substrates as object recognition ones, apart from the areas in the inferior temporal cortex already mentioned above.

However, the use of GLM and correlation of activities between areas are approaches with some serious limitations, because they are absolutely model driven. For example group clusters of areas as having similar task-related dynamics may be misleading, especially for the “accumulator” model. This happens because the response to the stimulus is always present. In any case, most visual areas decrease their activity upon prolonged exposure to the same stimulus, an effect known as adaptation. Furthermore, and in spite of the fact that stimulus presence and perceptual response are overlapped, which leads to overlapped predictors, this difficulty can be overcome by the separation of the times of onset of sensation and perception. This is a unique feature of our paradigm, which renders it a conceptual advantage over previous approaches, which were not able to separate onset of sensation from onset of perception [1]. Using this strategy we could identify areas relevant to the different stages of the decision process. Furthermore, we could control for low level features in stimulus images such as frequency content, spectral energy and luminosity.

In sum, we believe we have achieved the primary objective of this study which was identify the time moment at which rotation of Mooney face images affects electrical and BOLD brain activity, and used that information to dissect the neural correlates of decision.

5 - Future work

It is important to refine the analysis of EEG data, namely combining phase synchrony analysis with data-driven approaches. The study of inter-hemispheric relations in perceptual decision is also an important next step.

At this moment we are preparing an EEG/Eye tracker experiment with the same task as described here. This should reveal if artefacts are due to eye movements and clarify which face features (eyes, mouse, nose…) subjects use to discriminate Mooney faces.

In the future, we would also like to study similarities and differences between 2D and 3D face perception. We are now creating 3D Mooney faces from realistic 3D faces, in order to study how face discrimination and perceptual decision depend on face illumination or point of view.

Simultaneous recordings of EEG and fMRI will also be a future interesting step, because one can take advantage of the higher temporal resolution of EEG and spatial resolution of fMRI to better pinpoint the neural correlates of perceptual decision.

Future work, using EEG-informed fMRI should elucidate the role of the described circuits in more general object-processing.

Studies to verify stability and invariance of localizers under different task constraints are already being also performed.

Finally, we aim to explore novel ways of studying functional/structural connectivity to address the issues of necessity and causality of activation prior to decision. These techniques include diffusion tensor imaging (DTI[1]) and Granger Causality[2] approaches.

---

[1] DTI is a new brain imaging method which allows to study the complex networks of brain fibre connections between different brain areas, based on the movement of water molecules (along axons, white matter) in the brain by applying specific radio-frequency and magnetic field-gradient pulses. [84]

[2] Granger Causality is a concept based on prediction. According to Granger causality, if a signal X "granger-causes" another signal (Y), then the past values of the signal X may contain information that helps predict Y. In the last few years, with Granger causality, it has become possible to identify causal interactions in neural data and shed some light at the functional connectivity or network dynamics. [85]

Appendix

A. Channel clusters

Channel locations of each electrode set used to the more specific phase synchrony analysis.

OT	PT
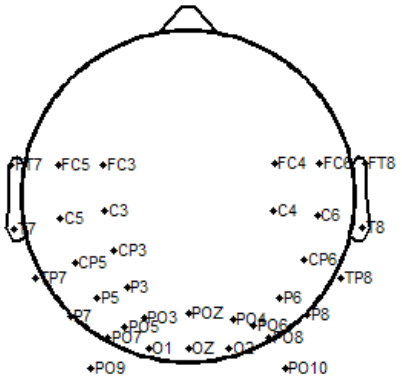	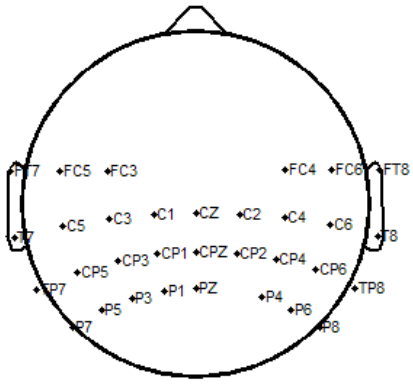
34 of 34 electrode locations shown	32 of 32 electrode locations shown
OF	**OP**
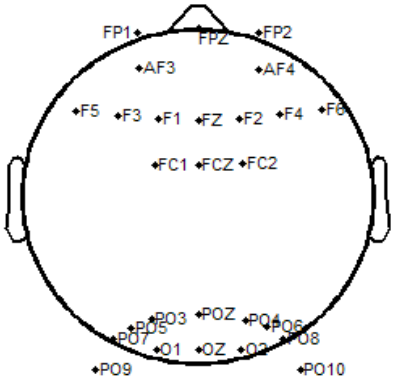	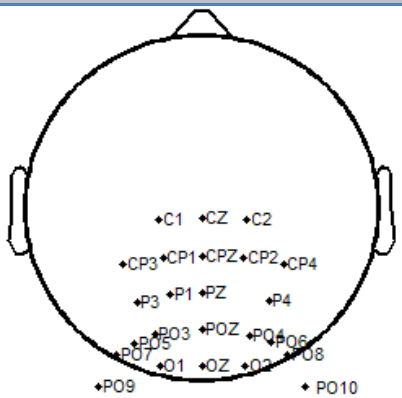
27 of 27 electrode locations shown	24 of 24 electrode locations shown

B. Analysis tree for EEG data

Here we represent the basic analysis tree. Two different approaches were carried out over EEG data and, for each one, specific filtering (e.g. Filt 15-100Hz), epoching (e.g. -2-1s), electrode clusters (e.g. 45-59 and OP) or baseline periods (e.g. BL -900- -600ms) were used.

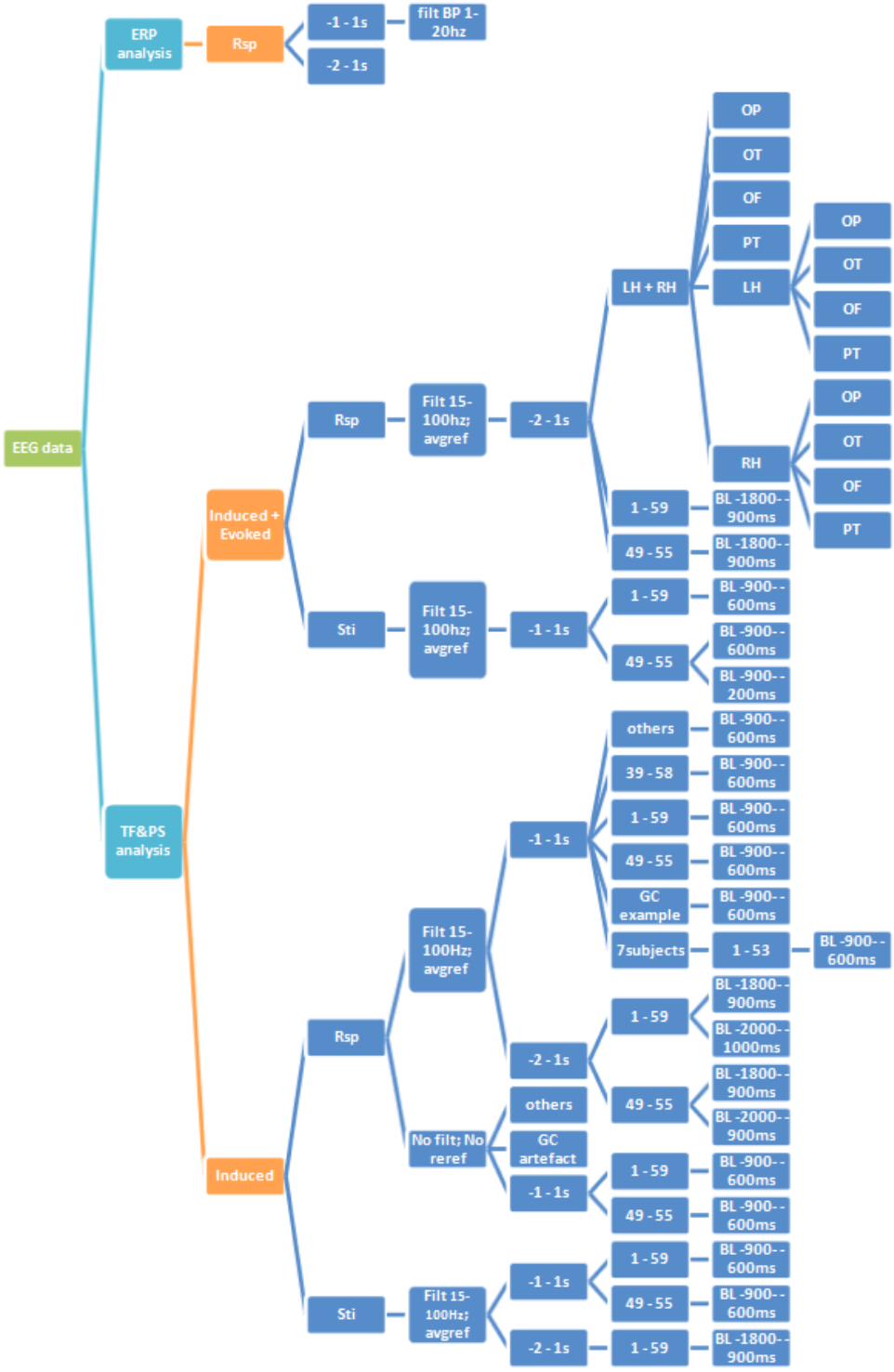

References

1. **McKeeff, T., Tong, F.** The Timing of Perceptual Decisions for Ambiguous Face Stimuli in the Human Ventral Visual Cortex. *Cerebral Cortex.* 2007, Vol. 17(3), pp. 669-678.

2. **Kanwisher, N., Yovel, G.** The fusiform face area: a cortical region specialized for the perception of faces. *Philos. Trans. R. Soc. Lond., B, Biol. Sci.* 2006, Vol. 361(1476), pp. 2109-2128.

3. **Gauthier, I., Williams, P., Tarr, M. J., Tanaka, J.** Training 'greeble' experts: a framework for studying expert object recognition processes. *Vision Res.* 1998, Vols. 38(15-16), pp. 2401-2428.

4. **Grill K., Kanwisher N.** The fusiform face area subserves face perception, not generic within-category identification. *Nature Neuroscience.* 2004, Vol. 7, pp. 555-562.

5. **Haxby, J., Hoffman, E., Gobbini, M.** The distributed human neural system for face perception. *Trends in Cognitive Sciences.* 2000, Vol. 4(6), pp. 223-233.

6. **Yovel, G., Kanwisher, N.** The neural basis of the behavioral face-inversion effect. *Curr. Biol.* 2005, Vol. 15(24), pp. 2256–2262.

7. **Rossion, B., Gauthier, I., Tarr, M. J., Despland, P., Bruyer, R., Linotte, S., et al.** The N170 occipito-temporal component is delayed and enchanced to inverted faces but not to inverted objects: an electorphysiological account of face-specific processes in the human brain. *Neuroreport.* 2000, Vol. 11(1), pp. 69-74.

8. **Latinus, M., Taylor, M. J.** Face processing stages: impact of difficulty and the separation of effects. *Brain Res.* 2006, Vol. 1123(1), pp. 179-187.

9. **Latinus, M., Taylor, M. J.** Holistic processing of faces: learning effects with Mooney faces. *J Cogn Neurosci.* 2005, Vol. 17(8), pp. 1316-1327.

10. **Trujillo, L. T., Peterson, M. A.** P100 and N170 ERP Components Reflect Differences Among Upright, Inverted, And Scrambled Mooney Faces . *Poster presented at the Annual Society for Neuroscience Meeting.* San Diego, California : s.n., October 2004.

11. **Summerfield, C., Egner, T., Greene, M., Koechlin, E.** Predictive codes for forthcoming perception in the frontal crotex. *Science.* 2006, Vol. 314(5803), pp. 1311-1314.

12. **Soon, C., Brass, M., Heinze, H., Haynes, J.** Brief Communications: Unconscious determinants of free decisions in the human brain. *Nature Neuroscience.* 2008, Vol. 11, pp. 543-545.

13. [Online] [Cited: 23 July 2008.] http://huehueteotl.wordpress.com/2008/04/15/decision-making-may-be-surprisingly-unconscious/.

14. **Fellows, Lesley K.** The Cognitive Neuroscience of Human Decision Making: A Review and Conceptual Framework Behav. *Cogn Neurosci Rev.* September 2004, Vol. 3, pp. 159 - 172.

15. **Krawczyk, Daniel C.** Contributions of the prefrontal cortex to the neural basis of human decision making. *Neurosci. Biobehav Rev.* 2002, Vol. 26(6), pp. 631-664.

16. **Phelps, E.A.** The cognitive neuroscience of emotion. [book auth.] M. S., Ivry, R. B., Mangun, G. R. Gazzaniga. *Cognitive Neuroscience: The Biology of Mind.* 2nd. NY : Norton, 2002.

17. **Mishkin, M., Ungerleider, L., & Macko, K.** Object vision and spatial vision: Two cortical pathways. *Trends in Neuroscience.* 1983, Vol. 6 , pp. 414-417.

18. **Milner, D. A., Goodale, M.** *The visual brain in action.* Oxford University Press, 1995.

19. **van Veen, V., Carter, C. S.** The anterior cingulate as a conflict monitor: fMRI and ERP studies. *Physiol Behav.* 2002, Vols. 77(4-5), pp. 477- 482.

20. **Cohen, M. X., Heller, A. S., Ranganath, C.** Functional connectivity with anterior cingulate and orbitofrontal cortices during decision-making. *Brain Res Cogn Brain Res.* 2005, pp. 61-70.

21. **Forstmann, B.U., Wolfensteller, U., Derrfuss, J., Neumann, J., Brass, M., et al.** When the Choice Is Ours: Context and Agency Modulate the Neural Bases of Decision-Making. *PLoS ONE.* 2008, Vol. 3.

22. **Chelazzi, L., Corbetta, M.** Cortical mechanisms of visuospatial attention in the primate brain. *The new cognitive neurosciences.* 2nd, 2000, pp. 667- 686.

23. **Kastner, S., Ungerleider, L. G.** Mechanisms of visual attention in the human cortex. *Annu Rev Neurosci.* 2000, Vol. 23, pp. 315-341.

24. [Online] [Cited: 16 July 2008.] http://www.memory-key.com/Neurology/glossary_brain.htm.

25. **Grossberg, S., Pilly, P. K.** Temporal dynamics of decision-making during motion perception in the visual cortex. *Vision Research.* 2008, Vol. 48(12), pp. 1345- 1373.

26. **Niedermeyer, E., Lopes da Silva, F.** *Electroencephalography: Basic Principles, Clinical Applications, and Related fields.* 5. Lippincott Williams & Wilkins, 2004.

27. [Online] [Cited: 22 April 2008.] http://www.mrc-cbu.cam.ac.uk/research/eeg/eeg_intro.html.

28. [Online] [Cited: 22 April 2008.] http://butler.cc.tut.fi/~malmivuo/bem/bembook/13/13.htm.

29. **Honda, Y., Watanabe, S., Nakamura, M., Miki, K., Kakigi, R.** Interhemispheric Difference for Upright and Inverted Face Perception in Humans: An Event-Related Potential Study. *Brain Topography.* 2007, Vol. 20(1), pp. 31-39.

30. **Teplan, M.** Fundamentals of EEG measurement. *Measurement Science Review.* 2002. Vol. 2, pp. 1-11.

31. **Fries, P., Scheeringa, R., Oostenveld, R.** Finding Gamma. *Neuron.* 2008, Vol. 58(3), pp. 303-305.

32. **Rodriguez, E., George, N., Lachaux, J., Martinerie, J., Renault, B., Varela, F.** Perception's shadow: long-distance synchronization of human brain activity. *Nature.* 1999, Vol. 397(6718), pp. 430-3.

33. **Brovelli, A., Daprati, E., Naranjo, R.H., Muzur, A., Longo, R., Battaglini, P.P.** A method for the discrimination between induced and evoked gamma band activity. *First International Conference on Advances in Medical Signal and Information Processin,.* 2000, pp. 226- 230.

34. **Tallon-Baudry, C.** Oscillatory synchrony and human visual cognition. *Journal of Physiology-Paris.* 2003, Vols. 97(2-3), pp. 355-363.

35. **Treisman, A.** The Binding problem. *Cognitive neuroscience.* 1996, Vol. 6, pp. 171- 178.

36. **Uhlhaas, P., Haenschel, C., Nikolic, D., Singer, W.** The Role of Oscillations and Synchrony in Cortical Networks and Their Putative Relevance for the Pathophysiology of Schizophrenia. *Schizophrenia Bulletin.* 2008, Vol. 34(5), pp. 927-943.

37. **Herrmann, C., Munk, M., Engel, A.** Cognitive functions of gamma-band activity: memory match and utilization. *Trends in Cognitive Sciences.* 2004, Vol. 8(8), pp. 347-355.

38. **Yuval-Greenberg, S., Tomer, O., Keren, A. S., Nelken, I., Deouell, L.Y.** Transient Induced Gamma-Band Response in EEG as a Manifestation of Miniature Saccades. *Neuron.* 2008, Vol. 58(3), pp. 429-441.

39. **Delorme, A., Fernsler, T., Serby, H., Makeig, S.** EEGLAB tutorial. California : University of San Diego, 2006.

40. **NeuroScan, Compumedics.** Scan 4.3 - Offline analysis of acquired data (Edit 4.3). USA : NeuroScan, 2003.

41. **Aunon, J., McGillem, C., Childers, D.** Signal processing in evoked potential research: averaging and modelling. *Crit. Rev. Bioeng.* 1981, Vol. 4, pp. 323-367.

42. **Buxton, Richard B.** *Introduction to Functional Magnetic Resonance Imaging: Principles and Techniques.* Cambridge University Press, 2002.

43. [Online] [Cited: 19 June 2008.] http://www.fmrib.ox.ac.uk/education/fmri/.

44. [Online] [Cited: 19 August 2008.] http://psychcentral.com/lib/2007/what-is-functional-magnetic-resonance-imaging-fmri/.

45. [Online] [Cited: 28 July 2008.] http://ccir.uhrad.com/sairc/mri.asp.

46. **Logothetis, N., Pauls, J., Augath, M., Trinath, T., Oeltermann, A.** Neurophysiological investigation of the basis of the fMRI signal. *Nature.* 2001, Vol. 412(6843), pp. 150-157.

47. [Online] [Cited: 26 August 2008.] http://uninews.unimelb.edu.au/view.php?articleID=3623.

48. **Uhlhaas, P., Linden, D., Singer, W., Haenschel, C., Lindner, M., Maurer, K., Rodriguez, E.** Dysfunctional Long-Range Coordination of Neural Activity during Gestalt Perception in Schizophrenia. *J. Neurosci.* 2006, Vol. 26(31), pp. 8168–8175.

49. [Online][Cited: 8 January 2008.] http://www.princeton.edu/~artofsci/gallery/view.php%3Fid=77.html

50. **Kanwisher, N., Tong, F., Nakayama, K.** The effect of face inversion on the human fusiform face area. *Cognition.* 1998, Vol. 68(1), pp. B1-B11.

51. **Huettel, S.** Issues in Experimental Design. Durham North Carolina, USA , 2002. Brain Imaging and Analysis Center: fMRI Graduate Course.

52. **Lorist, M.M., Klein, M., Nieuwenhuis, S., De Jong, R., Mulder, G., Meijman, T.F.** Mental fatigue and task control: Planning and preparation. *Psychophysiology*. 2000, Vol. 37(5), pp. 614-625.

53. **Lachaux, J., Rodriguez, E., Martinerie, J., Varela, F.** Measuring Phase Synchrony in Brain Signals. *Human Brain Mapping.* 1999, Vol. 8(4), pp. 194-208.

54. [Online] [Cited: 27 August 2008.] http://www.nordicneurolab.com.

55. **Ploran, E., Nelson, S., Velanova, K., Donaldson, D., Petersen, S., Wheeler, M.** Evidence Accumulation and the Moment of Recognition: Dissociating Perceptual Recognition Processes Using fMRI. *J. Neurosci.* 2007, Vol. 27(44), pp. 11912-24.

56. **Castelo-Branco, M., Neuenschwander, S., Singer W.** Synchronization of Visual Responses between the Cortex, Lateral Geniculate Nucleus, and Retina in the Anesthetized Cat. *J. Neurosci.* 1998, Vol. 18, pp. 6395-6410.

57. **Elliott, R., Dolan, R. J., Frith, C. D.** Dissociable functions in the medial and lateral orbitofrontal cortex: evidence from human neuroimaging studies. *Cereb Cortex.* 2000, Vol. 10, pp. 308- 317.

58. **Fox, CJ., Iaria, G., Barton, JJ.** Disconnection in prosopagnosia and face processing. *Cortex.* 2008, Vol. 44(8), pp. 996-1009.

59. **Kanwisher, N., McDermott, J., Chun, M.** The fusiform face area: a module in human extrastriate cortex specialized for face perception. *J. Neurosci.* 1997, Vol. 17(11), pp. 4302-4311.

60. **Grill-Spector, K.** The neural basis of object perception. *Current Opinion in Neurobiology.* 2003, Vol. 13(2), pp. 159-166.

61. **Kriegeskorte, N., Formisano, E., Sorger, B., Goebel, R.** Individual faces elicit distinct response patterns in human anterior temporal cortex. *Proc. Natl. Acad. Sci. USA.* 2007, Vol. 104(51), pp. 20600-5.

62. **Haxby, J., Gobbini, M., Furey, M., Ishai, A., Schouten, J., Pietrini, P.** Distributed and overlapping representations of faces and objects in ventral temporal cortex. *Science.* 2001, Vol. 293, pp. 2425-2430.

63. **Buckner, RL., Andrews-Hanna, JR., Schacter, DL.** The brain's default network: anatomy, function, and relevance to disease. *Ann N Y Acad Sci.* 2008, Vol. 1124, pp. 1-38.

64. **Yin, R.** Looking at upside-down faces. *Journal of Experimental Psychology: General.* 1969, Vol. 81, pp. 141-145.

65. **Valentine, T.** Upside-down faces: a review of the effects of inversion upon face recognition. *British Journal of Psycology.* 1988, Vol. 79(Pt 4), pp. 471-491.

66. **Farah, J., Takana, W., Drain, M.** What causes the face inversion effect? *Journal of Experimental Psychology: Human Perception and Performance.* 1995, Vol. 21, pp. 628-634.

67. **Farah, J., Wilson, W., Drain, M., Takana, N.** What is special about face perception? *Psychological Review.* 1998, Vol. 105, pp. 482-498.

68. **Riesenhuber, M., Jarudi, I., Gilad, S., Sinha, P.** Face processing in humans is compatible with a simple shape-based model of vision. *Biological Sciences.* 2004, Vol. 271, pp. 448-450.

69. **Boutet, I., Chaudhuri, A.** Multistability of overlapped face stimuli is dependent upon orientation. *Perception.* 2001, Vol. 30(6), pp. 743-753.

70. **McKone, E.** Isolating the special component of face recognition: peripheral identification and a Mooney face. *Journal of Experimental Psychology: Learning, Memory and Cognition.* 2004, Vol. 30(1), pp. 181-197.

71. **Murray, J. E., Yong, E., Rhodes, G.** Revisiting the perception of upside-down faces. *Psychological Science.* 2000, Vol. 11(6), pp. 492-496.

72. **Rossion, B., Boremanse, A.** Nonlinear relationship between holistic processing of individual faces and picture-plane rotation: Evidence from the face composite illusion. *Journal of Vision.* 2008, Vol. 8(4), pp. 1-13.

73. **Schwaninger, A., Mast, F.** Why is face recognition so orientation-sensitive? Psychophysical evidence for an integrative model. *Perception.* 1999, Vol. 28 (Supplement), p. 116.

74. **Sturzel, F., Spillmann, L.** Thatcher illusion: dependence on angle of rotation. *Perception.* 2000, Vol. 29(8), pp. 937-942.

75. **Valentine, T., Bruce, V.** Mental rotation of faces. *Memory and Cognition.* 1988, Vol. 16(6), pp. 556-566.

76. **Yovel, G., Kanwisher, N.** Face perception domain specific, not process specific. *Neuron.* 2004, Vol. 44(5), pp. 889-898.

77. **Haxby, J. V., Ungerleider, L. G., Clark, V. P., Schouten, J. L., Hoffman, E. A., Martin, A.** The effect of face inversion on activity in human neural systems for face and object perception. *Neuron.* 1999, Vol. 22(1), pp. 189-199.

78. **Rossion, B., Joyce, C. A., Cottrell, G. W., Tarr, M. J.** Early lateralization and orientation tuning for face, word, and object processing in the visual cortex. *Neuroimage.* 2003, Vol. 20(3), pp. 1609-1624.

79. **Botzel, K., Grusser, J.** Electric brain potentials evoked by pictures of faces and non-faces: a search for 'face-specific' EEG-potentials. *Experimental Brain Research.* 1989, Vol. 77(2), pp. 349-360.

80. **Jeffreys, D. A.** Evoked potentials studies of face and object processing. *Visual Cognition.* 1996, Vol. 3(1), pp. 1-38.

81. **Itier, R. L., Taylor, M. J.** N170 or N1? Spatiotemporal differences between object and face processing using ERPs. *Cerebral Cortex.* 2004, Vol. 14(2), pp. 132-142.

82. **Itier, R. L., Taylor, M. J.** Inversion and contrast polarity reversal affect both enconding and recognition processes of unfamiliar faces: a repetition study using ERPs. *Neuroimage.* 2002, Vol. 15(2), pp. 353-372.

83. **Jacques, C., Rossion, B.** Early electrophysiological responses to multiple face orientations correlate with individual discrimination performance in humans. *Neuroimage.* 2007, Vol. 36(3), pp. 863-876.

84. [Online] [Cited: 8 July 2008.] http://www.technologyreview.com/article/16473/page1/.

85. **Roebroeck, A., Formisano, E., Goebel, R.** Mapping directed influence over the brain using granger causality mapping. *Neuroimage.* 2005, Vol. 25(1), pp. 230-242.